

Testing leptoquark models in $\bar{B} \rightarrow D^{(*)} \tau \bar{\nu}$

Yasuhito Sakaki* and Ryoutaro Watanabe†

Theory Group, IPNS, KEK, Tsukuba, Ibaraki 305-0801, Japan

Minoru Tanaka‡ and Andrey Tayduganov§

Department of Physics, Graduate School of Science, Osaka University, Toyonaka, Osaka 560-0043, Japan
 (Received 9 September 2013; published 14 November 2013)

We study potential new physics effects in the $\bar{B} \rightarrow D^{(*)} \tau \bar{\nu}$ decays. As a particular example of new physics models, we consider the class of leptoquark models and put the constraints on the leptoquark couplings using the recently measured ratios $R(D^{(*)}) = \mathcal{B}(\bar{B} \rightarrow D^{(*)} \tau \bar{\nu}) / \mathcal{B}(\bar{B} \rightarrow D^{(*)} \mu \bar{\nu})$. For consistency, some of the constraints are compared with the ones coming from the current experimental bound on $\mathcal{B}(B \rightarrow X_s \nu \bar{\nu})$. In order to discriminate various new physics scenarios, we examine the correlations between different observables that can be measured in the future.

 DOI: [10.1103/PhysRevD.88.094012](https://doi.org/10.1103/PhysRevD.88.094012)

PACS numbers: 13.20.-v, 13.20.He, 14.80.Sv

I. INTRODUCTION

An excess of exclusive semitauonic decays of the B meson, $\bar{B} \rightarrow D^{(*)} \tau \bar{\nu}$, has been reported by the *BABAR* and *Belle* collaborations. In order to test the lepton universality with less theoretical uncertainty, the ratios of the branching fractions are introduced as observables,

$$R(D^{(*)}) \equiv \frac{\mathcal{B}(\bar{B} \rightarrow D^{(*)} \tau \bar{\nu})}{\mathcal{B}(\bar{B} \rightarrow D^{(*)} \ell \bar{\nu})}, \quad (1)$$

where ℓ denotes e or μ . The present experimental results coming from the *BABAR* experiment are given by [1,2]

$$R(D)^{BABAR} = 0.440 \pm 0.072, \quad R(D^*)^{BABAR} = 0.332 \pm 0.030, \quad (2)$$

with their correlation $\rho = -0.27$, where the statistical and systematical errors are combined assuming Gaussian distribution. For the corresponding results from several *Belle* publications [3–5], we combine the results that have the smallest errors for each charge mode, and obtain the following numbers:

$$R(D)^{Belle} = 0.390 \pm 0.100, \quad R(D^*)^{Belle} = 0.347 \pm 0.050, \quad (3)$$

where the unknown correlation is assumed to be zero in this case. Further combining Eqs. (2) and (3), we obtain

$$R(D) = 0.421 \pm 0.058, \quad R(D^*) = 0.337 \pm 0.025, \quad (4)$$

with the correlation to be -0.19 . Comparing these experimental results with the Standard Model (SM) predictions,

$$R(D)^{SM} = 0.305 \pm 0.012, \quad R(D^*)^{SM} = 0.252 \pm 0.004, \quad (5)$$

we find that the discrepancy is 3.5σ combining $R(D)$ and $R(D^*)$.

From the theoretical point of view, the two-Higgs-doublet model of type II (2HDM-II) [6], which is the Higgs sector of the minimal supersymmetric Standard Model (MSSM) [7], has been studied well in the literature [8–12] as a candidate of new physics (NP) that significantly affects the semitauonic B decays. Based on these theoretical works and their experimental data, the *BABAR* Collaboration shows that the 2HDM-II is excluded at 99.8% confidence level (C.L.) [1,2].

This observation has stimulated further theoretical activities for clarifying the origin of the above discrepancy. Several authors have studied various NP scenarios other than 2HDM-II. Possible structures of the relevant four-fermion interaction are identified and models that induce such structures are proposed in the literature [13–22]. One of the interesting four-fermion operators is the scalar type generated in the 2HDMs with flavor changing neutral currents, the so-called 2HDM of type III [23]. It is shown that this operator, mentioned as $\mathcal{O}_{S_2}^l$ below, explains the experimental data. Another compelling possibility is the tensor operator \mathcal{O}_T^l . Two of us have shown that \mathcal{O}_T^l describes the present experimental results with a reasonable range of its Wilson coefficient and predicts τ and D^* polarizations different from $\mathcal{O}_{S_2}^l$ [24]. They have also studied a leptoquark model as an intriguing example that induces these operators. The effect of the tensor operator also has been studied recently in Ref. [25] in a model-independent way and in Ref. [26] in leptoquark models.

In this work, we extend the analysis in Ref. [24] to all possible leptoquark models [27]. It is shown that three of them explain the present experimental data quite well. In our study, we carefully investigate theoretical uncertainty in the evaluation of NP contributions in $\bar{B} \rightarrow D^{(*)} \tau \bar{\nu}$ by employing two different sets of relevant hadronic form factors. The rest of the paper is organized as follows. The effective Hamiltonian including all possible four-fermion operators, the relevant helicity amplitudes of $\bar{B} \rightarrow D^{(*)} \tau \bar{\nu}$,

*sakakiy@post.kek.jp

†wryou@post.kek.jp

‡tanaka@phys.sci.osaka-u.ac.jp

§tayduganov@het.phys.sci.osaka-u.ac.jp

and the analytic formulas of differential decay rates are presented in Sec. II. After introducing all possible leptoquark models, we evaluate Wilson coefficients of the effective Hamiltonian in Sec. III. Constraints from $\bar{B} \rightarrow D^{(*)}\tau\bar{\nu}$ as well as those from $\bar{B} \rightarrow X_s\nu\bar{\nu}$ are also shown in Sec. III. Section III also contains a discussion on theoretical uncertainty in the constraints from $\bar{B} \rightarrow D^{(*)}\tau\bar{\nu}$. In Sec. IV we study all possible correlations between various observables in order to distinguish different NP models. Section V is devoted to our conclusions. Some details of hadronic form factors and decay distributions are relegated to appendixes.

II. EFFECTIVE HAMILTONIAN AND HELICITY AMPLITUDES

Assuming the neutrinos to be left-handed, we introduce the most general effective Hamiltonian that contains all possible four-fermion operators of the lowest dimension for the $b \rightarrow c\tau\bar{\nu}_l$ transition,

$$\begin{aligned} \frac{d\Gamma(\bar{B} \rightarrow D\tau\bar{\nu}_l)}{dq^2} &= \frac{G_F^2 |V_{cb}|^2}{192\pi^3 m_B^3} q^2 \sqrt{\lambda_D(q^2)} \left(1 - \frac{m_\tau^2}{q^2}\right)^2 \times \left\{ |\delta_{l\tau} + C_{V_1}^l + C_{V_2}^l|^2 \left[\left(1 + \frac{m_\tau^2}{2q^2}\right) H_{V,0}^{s2} + \frac{3}{2} \frac{m_\tau^2}{q^2} H_{V,t}^{s2} \right] \right. \\ &+ \frac{3}{2} |C_{S_1}^l + C_{S_2}^l|^2 H_S^{s2} + 8 |C_T^l|^2 \left(1 + \frac{2m_\tau^2}{q^2}\right) H_T^{s2} + 3 \mathcal{R}e[(\delta_{l\tau} + C_{V_1}^l + C_{V_2}^l)(C_{S_1}^{l*} + C_{S_2}^{l*})] \frac{m_\tau}{\sqrt{q^2}} H_S^s H_{V,t}^s \\ &\left. - 12 \mathcal{R}e[(\delta_{l\tau} + C_{V_1}^l + C_{V_2}^l) C_T^{l*}] \frac{m_\tau}{\sqrt{q^2}} H_T^s H_{V,0}^s \right\}, \end{aligned} \quad (8)$$

and

$$\begin{aligned} \frac{d\Gamma(\bar{B} \rightarrow D^*\tau\bar{\nu}_l)}{dq^2} &= \frac{G_F^2 |V_{cb}|^2}{192\pi^3 m_B^3} q^2 \sqrt{\lambda_{D^*}(q^2)} \left(1 - \frac{m_\tau^2}{q^2}\right)^2 \\ &\times \left\{ (|\delta_{l\tau} + C_{V_1}^l|^2 + |C_{V_2}^l|^2) \left[\left(1 + \frac{m_\tau^2}{2q^2}\right) (H_{V,+}^2 + H_{V,-}^2 + H_{V,0}^2) + \frac{3}{2} \frac{m_\tau^2}{q^2} H_{V,t}^2 \right] \right. \\ &- 2 \mathcal{R}e[(\delta_{l\tau} + C_{V_1}^l) C_{V_2}^{l*}] \left[\left(1 + \frac{m_\tau^2}{2q^2}\right) (H_{V,0}^2 + 2H_{V,+} + H_{V,-}) + \frac{3}{2} \frac{m_\tau^2}{q^2} H_{V,t}^2 \right] \\ &+ \frac{3}{2} |C_{S_1}^l - C_{S_2}^l|^2 H_S^2 + 8 |C_T^l|^2 \left(1 + \frac{2m_\tau^2}{q^2}\right) (H_{T,+}^2 + H_{T,-}^2 + H_{T,0}^2) \\ &+ 3 \mathcal{R}e[(\delta_{l\tau} + C_{V_1}^l - C_{V_2}^l)(C_{S_1}^{l*} - C_{S_2}^{l*})] \frac{m_\tau}{\sqrt{q^2}} H_S H_{V,t} \\ &- 12 \mathcal{R}e[(\delta_{l\tau} + C_{V_1}^l) C_T^{l*}] \frac{m_\tau}{\sqrt{q^2}} (H_{T,0} H_{V,0} + H_{T,+} H_{V,+} - H_{T,-} H_{V,-}) \\ &\left. + 12 \mathcal{R}e[C_{V_2}^l C_T^{l*}] \frac{m_\tau}{\sqrt{q^2}} (H_{T,0} H_{V,0} + H_{T,+} H_{V,-} - H_{T,-} H_{V,+}) \right\}, \end{aligned} \quad (9)$$

where $\lambda_{D^{(*)}}(q^2) = ((m_B - m_{D^{(*)}})^2 - q^2)((m_B + m_{D^{(*)}})^2 - q^2)$.

The hadronic amplitudes in $\bar{B} \rightarrow M\tau\bar{\nu}_l$ ($M = D, D^*$) are defined as

$$\begin{aligned} H_{V_{1,2},\lambda}^{\lambda_M}(q^2) &= \varepsilon_\mu^*(\lambda) \langle M(\lambda_M) | \bar{c} \gamma^\mu (1 \mp \gamma_5) b | \bar{B} \rangle, & H_{S_{1,2},\lambda}^{\lambda_M}(q^2) &= \langle M(\lambda_M) | \bar{c} (1 \pm \gamma_5) b | \bar{B} \rangle, \\ H_{T,\lambda\lambda'}^{\lambda_M}(q^2) &= -H_{T,\lambda'\lambda}^{\lambda_M}(q^2) = \varepsilon_\mu^*(\lambda) \varepsilon_\nu^*(\lambda') \langle M(\lambda_M) | \bar{c} \sigma^{\mu\nu} (1 - \gamma_5) b | \bar{B} \rangle, \end{aligned} \quad (10)$$

$$\begin{aligned} \mathcal{H}_{\text{eff}} &= \frac{4G_F}{\sqrt{2}} V_{cb} [(\delta_{l\tau} + C_{V_1}^l) \mathcal{O}_{V_1}^l + C_{V_2}^l \mathcal{O}_{V_2}^l \\ &+ C_{S_1}^l \mathcal{O}_{S_1}^l + C_{S_2}^l \mathcal{O}_{S_2}^l + C_T^l \mathcal{O}_T^l], \end{aligned} \quad (6)$$

with the operator basis defined as

$$\begin{aligned} \mathcal{O}_{V_1}^l &= (\bar{c}_L \gamma^\mu b_L)(\bar{\tau}_L \gamma_\mu \nu_{lL}), & \mathcal{O}_{V_2}^l &= (\bar{c}_R \gamma^\mu b_R)(\bar{\tau}_L \gamma_\mu \nu_{lL}), \\ \mathcal{O}_{S_1}^l &= (\bar{c}_L b_R)(\bar{\tau}_R \nu_{lL}), & \mathcal{O}_{S_2}^l &= (\bar{c}_R b_L)(\bar{\tau}_R \nu_{lL}), \\ \mathcal{O}_T^l &= (\bar{c}_R \sigma^{\mu\nu} b_L)(\bar{\tau}_R \sigma_{\mu\nu} \nu_{lL}). \end{aligned} \quad (7)$$

Since the neutrino flavor l is not determined experimentally in B decays, we consider $l = e, \mu$ or τ . In the SM, the Wilson coefficients are set to zero, $C_X^l = 0$ ($X = V_{1,2}, S_{1,2}, T$).

Using this effective Hamiltonian in Eq. (6) and calculating the helicity amplitudes (for the details see Ref. [24]), one finds the differential decay rates as follows:

where λ_M and λ denote the meson and virtual intermediate boson helicities ($\lambda_M = s$ and $\lambda_M = 0, \pm 1$ for D and D^* , respectively, and $\lambda = 0, \pm 1, t$) in the B rest frame, respectively. A detailed description of the matrix elements can be found in Appendix A. The nonzero amplitudes are given below.

(i) $\bar{B} \rightarrow D\tau\bar{\nu}$:

$$H_{V,0}^s(q^2) \equiv H_{V_{1,0}}^s(q^2) = H_{V_{2,0}}^s(q^2) = \sqrt{\frac{\lambda_D(q^2)}{q^2}} F_1(q^2), \quad (11a)$$

$$H_{V,t}^s(q^2) \equiv H_{V_{1,t}}^s(q^2) = H_{V_{2,t}}^s(q^2) = \frac{m_B^2 - m_D^2}{\sqrt{q^2}} F_0(q^2), \quad (11b)$$

$$H_S^s(q^2) \equiv H_{S_1}^s(q^2) = H_{S_2}^s(q^2) \simeq \frac{m_B^2 - m_D^2}{m_b - m_c} F_0(q^2), \quad (11c)$$

$$H_T^s(q^2) \equiv H_{T,+}^s(q^2) = H_{T,0}^s(q^2) = -\frac{\sqrt{\lambda_D(q^2)}}{m_B + m_D} F_T(q^2). \quad (11d)$$

(ii) $\bar{B} \rightarrow D^*\tau\bar{\nu}$:

$$H_{V,\pm}(q^2) \equiv H_{V_{1,\pm}}^\pm(q^2) = -H_{V_{2,\mp}}^\mp(q^2) = (m_B + m_{D^*})A_1(q^2) \mp \frac{\sqrt{\lambda_{D^*}(q^2)}}{m_B + m_{D^*}} V(q^2), \quad (12a)$$

$$H_{V,0}(q^2) \equiv H_{V_{1,0}}^0(q^2) = -H_{V_{2,0}}^0(q^2) = \frac{m_B + m_{D^*}}{2m_{D^*}\sqrt{q^2}} \left[-(m_B^2 - m_{D^*}^2 - q^2)A_1(q^2) + \frac{\lambda_{D^*}(q^2)}{(m_B + m_{D^*})^2} A_2(q^2) \right], \quad (12b)$$

$$H_{V,t}(q^2) \equiv H_{V_{1,t}}^0(q^2) = -H_{V_{2,t}}^0(q^2) = -\sqrt{\frac{\lambda_{D^*}(q^2)}{q^2}} A_0(q^2), \quad (12c)$$

$$H_S(q^2) \equiv H_{S_1}^0(q^2) = -H_{S_2}^0(q^2) \simeq -\frac{\sqrt{\lambda_{D^*}(q^2)}}{m_b + m_c} A_0(q^2), \quad (12d)$$

$$H_{T,\pm}(q^2) \equiv \pm H_{T,\pm t}^\pm(q^2) = \frac{1}{\sqrt{q^2}} \left[\pm(m_B^2 - m_{D^*}^2)T_2(q^2) + \sqrt{\lambda_{D^*}(q^2)}T_1(q^2) \right], \quad (12e)$$

$$H_{T,0}(q^2) \equiv H_{T,+}^0(q^2) = H_{T,0}^0(q^2) = \frac{1}{2m_{D^*}} \left[-(m_B^2 + 3m_{D^*}^2 - q^2)T_2(q^2) + \frac{\lambda_{D^*}(q^2)}{m_B^2 - m_{D^*}^2} T_3(q^2) \right]. \quad (12f)$$

In Eqs. (11c) and (12d), the equations of motion are used for the quark fields.

Up to now all experimental and phenomenological analyses of $\bar{B} \rightarrow D^{(*)}\tau\bar{\nu}$ decays have been made highly relying on the heavy quark effective theory (HQET). Although it provides an extremely useful tool in describing the nonperturbative dynamics of QCD, an alternative description of these decays that does not rely on HQET is welcome. Therefore, in order to be conservative and to estimate the sensitivity of NP constraints to the $\bar{B} \rightarrow D^{(*)}$ transition matrix elements, two different sets of hadronic form factors are examined:

- (i) HQET form factors, parametrized by Caprini *et al.* [28] with the use of parameters extracted from experiments by the *BABAR* and *Belle* collaborations;
- (ii) form factors, computed by Melikhov and Stech (MS) using a relativistic dispersion approach based on the constituent quark model [29].

III. TESTING LEPTOQUARK MODELS

A. Effective Lagrangian and Wilson coefficients

Many extensions of the SM, motivated by a unified description of quarks and leptons, predict the existence of new scalar and vector bosons, called leptoquarks, which decay into a quark and a lepton (with a model-dependent branching fraction). These particles carry nonzero baryon and lepton numbers, color, and fractional electric charge.

Although for the leptoquark masses that are within experimental reach at collider experiments, the flavor-changing neutral current (FCNC) processes favor leptoquarks that couple to quarks and leptons of the same generation, in this work we study the leptoquarks which couple to the third and the second generation. We use the Lagrangian with the general dimensionless $SU(3)_c \times SU(2)_L \times U(1)_Y$ invariant *flavor nondiagonal* couplings of scalar and vector leptoquarks satisfying baryon and

lepton number conservation, introduced by Buchmüller *et al.* [27]. The interaction Lagrangian that induces contributions to the $b \rightarrow c\ell\bar{\nu}$ process is given as follows:

$$\begin{aligned}\mathcal{L}^{\text{LQ}} &= \mathcal{L}_{F=0}^{\text{LQ}} + \mathcal{L}_{F=-2}^{\text{LQ}}, \\ \mathcal{L}_{F=0}^{\text{LQ}} &= (h_{1L}^{ij}\bar{Q}_{iL}\gamma^\mu L_{jL} + h_{1R}^{ij}\bar{d}_{iR}\gamma^\mu \ell_{jR})U_{1\mu} \\ &\quad + h_{3L}^{ij}\bar{Q}_{iL}\boldsymbol{\sigma}\gamma^\mu L_{jL}U_{3\mu} \\ &\quad + (h_{2L}^{ij}\bar{u}_{iR}L_{jL} + h_{2R}^{ij}\bar{Q}_{iL}i\sigma_2\ell_{jR})R_2, \\ \mathcal{L}_{F=-2}^{\text{LQ}} &= (g_{1L}^{ij}\bar{Q}_{iL}i\sigma_2L_{jL} + g_{1R}^{ij}\bar{u}_{iR}^c\ell_{jR})S_1 \\ &\quad + g_{3L}^{ij}\bar{Q}_{iL}i\sigma_2\boldsymbol{\sigma}L_{jL}S_3 \\ &\quad + (g_{2L}^{ij}\bar{d}_{iR}\gamma^\mu L_{jL} + g_{2R}^{ij}\bar{Q}_{iL}\gamma^\mu \ell_{jR})V_{2\mu},\end{aligned}\quad (13)$$

where Q_i and L_j are the left-handed quark and lepton $SU(2)_L$ doublets, respectively, while u_{iR} , d_{iR} , and ℓ_{jR} are the right-handed up, down quark and charged lepton $SU(2)_L$ singlets; indices i and j denote the generations of quarks and leptons; and $\psi^c = C\bar{\psi}^T = C\gamma^0\psi^*$ is a charge-conjugated fermion field. For simplicity, the color indices

TABLE I. Quantum numbers of scalar and vector leptoquarks with $SU(3)_c \times SU(2)_L \times U(1)_Y$ invariant couplings.

	S_1	S_3	V_2	R_2	U_1	U_3
spin	0	0	1	0	1	1
$F = 3B + L$	-2	-2	-2	0	0	0
$SU(3)_c$	3*	3*	3*	3	3	3
$SU(2)_L$	1	3	2	2	1	3
$U(1)_{Y=Q-T_3}$	1/3	1/3	5/6	7/6	2/3	2/3

are suppressed. The quantum numbers of the leptoquarks are summarized in Table I.

We note that *the fermion fields in Eq. (13) are given in the gauge eigenstate basis in which Yukawa couplings of the up-type quarks and the charged leptons are diagonal.* Rotating the down-type quark fields into the mass eigenstate basis and performing the Fierz transformations, one finds the general Wilson coefficients *at the leptoquark mass scale* for all possible types of leptoquarks contributing to the $b \rightarrow c\tau\bar{\nu}_l$ process:

$$C_{V_1}^l = \frac{1}{2\sqrt{2}G_F V_{cb}} \sum_{k=1}^3 V_{k3} \left[\frac{g_{1L}^{kl}g_{1L}^{23*}}{2M_{S_1^{1/3}}^2} - \frac{g_{3L}^{kl}g_{3L}^{23*}}{2M_{S_3^{1/3}}^2} + \frac{h_{1L}^{2l}h_{1L}^{k3*}}{M_{U_1^{2/3}}^2} - \frac{h_{3L}^{2l}h_{3L}^{k3*}}{M_{U_3^{2/3}}^2} \right], \quad (14a)$$

$$C_{V_2}^l = 0, \quad (14b)$$

$$C_{S_1}^l = \frac{1}{2\sqrt{2}G_F V_{cb}} \sum_{k=1}^3 V_{k3} \left[-\frac{2g_{2L}^{kl}g_{2R}^{23*}}{M_{V_2^{1/3}}^2} - \frac{2h_{1L}^{2l}h_{1R}^{k3*}}{M_{U_1^{2/3}}^2} \right], \quad (14c)$$

$$C_{S_2}^l = \frac{1}{2\sqrt{2}G_F V_{cb}} \sum_{k=1}^3 V_{k3} \left[-\frac{g_{1L}^{kl}g_{1R}^{23*}}{2M_{S_1^{1/3}}^2} - \frac{h_{2L}^{2l}h_{2R}^{k3*}}{2M_{R_2^{2/3}}^2} \right], \quad (14d)$$

$$C_T^l = \frac{1}{2\sqrt{2}G_F V_{cb}} \sum_{k=1}^3 V_{k3} \left[\frac{g_{1L}^{kl}g_{1R}^{23*}}{8M_{S_1^{1/3}}^2} - \frac{h_{2L}^{2l}h_{2R}^{k3*}}{8M_{R_2^{2/3}}^2} \right], \quad (14e)$$

where V_{k3} denotes the Cabibbo-Kobayashi-Maskawa matrix elements and the upper index of the leptoquark denotes its electric charge. In the following we will neglect double Cabibbo suppressed $\mathcal{O}(\lambda^2)$ terms and keep only the leading terms proportional to $V_{33} \equiv V_{tb}$.

The vector and axial vector currents are not renormalized and their anomalous dimensions vanish. The scale dependence of the scalar and tensor currents at leading logarithm approximation is given by

$$\begin{aligned}C_S(\mu_b) &= \left[\frac{\alpha_s(m_t)}{\alpha_s(\mu_b)} \right]^{2\beta_0^{\gamma_S}} \left[\frac{\alpha_s(m_{\text{LQ}})}{\alpha_s(m_t)} \right]^{2\beta_0^{\gamma_S(6)}} C_S(m_{\text{LQ}}), \\ C_T(\mu_b) &= \left[\frac{\alpha_s(m_t)}{\alpha_s(\mu_b)} \right]^{2\beta_0^{\gamma_T}} \left[\frac{\alpha_s(m_{\text{LQ}})}{\alpha_s(m_t)} \right]^{2\beta_0^{\gamma_T(6)}} C_T(m_{\text{LQ}}),\end{aligned}\quad (15)$$

where the anomalous dimensions of the scalar and tensor operators are $\gamma_S = -6C_F = -8$, $\gamma_T = 2C_F = 8/3$, respectively, and $\beta_0^{(f)} = 11 - 2n_f/3$ [26]. Taking into account the

most recent constraints on the scalar and vector leptoquark masses by the ATLAS and CMS collaborations [30,31], in our numerical analysis we assume that all scalar and vector leptoquarks are of the same mass $m_{\text{LQ}} = 1$ TeV. The b -quark scale is chosen to be $\mu_b = \bar{m}_b = 4.2$ GeV.

One can easily notice from Eq. (14) that in the simplified scenario with a presence of only one type of leptoquark, namely, $R_2^{2/3}$ or $S_1^{1/3}$, the scalar $C_{S_2}^l$ and tensor C_T^l Wilson coefficients are no longer independent: one finds that at the scale of leptoquark mass $C_{S_2}^l(m_{\text{LQ}}) = \pm 4C_T^l(m_{\text{LQ}})$. Then, using Eq. (15), one obtains the relation at the bottom mass scale,

$$C_{S_2}^l(\bar{m}_b) \simeq \pm 7.8C_T^l(\bar{m}_b). \quad (16)$$

B. Constraints from $\bar{B} \rightarrow X_s \nu \bar{\nu}$

Recent progress in experiment and theory has made FCNCs in B decays good tests of the SM and powerful

probes of NP beyond the SM. Along with the $b \rightarrow s\gamma$ and $b \rightarrow s\ell^+\ell^-$ processes, the $b \rightarrow s\nu\bar{\nu}$ decay is also sensitive to extensions of the SM. From a theoretical point of view, the inclusive decay $\bar{B} \rightarrow X_s\nu\bar{\nu}$ is a very clean process since both perturbative α_s and nonperturbative $1/m_b^2$ corrections are known to be small, what makes it to be well suited to search for NP.

The $b \rightarrow s\nu_j\bar{\nu}_i$ process can be described by the following effective Hamiltonian:

$$\mathcal{H}_{\text{eff}} = \frac{4G_F}{\sqrt{2}} V_{tb} V_{ts}^* [(\delta_{ij} C_L^{\text{SM}} + C_L^{ij}) \mathcal{O}_L^{ij} + C_R^{ij} \mathcal{O}_R^{ij}], \quad (17)$$

where the left- and right-handed operators are defined as

$$\begin{aligned} \mathcal{O}_L^{ij} &= (\bar{s}_L \gamma^\mu b_L)(\bar{\nu}_{jL} \gamma_\mu \nu_{iL}), \\ \mathcal{O}_R^{ij} &= (\bar{s}_R \gamma^\mu b_R)(\bar{\nu}_{jL} \gamma_\mu \nu_{iL}). \end{aligned} \quad (18)$$

In the SM, the Wilson coefficient is determined by box and Z-penguin loop diagrams computation which gives

$$C_L^{\text{SM}} = \frac{\alpha}{2\pi \sin^2 \theta_W} X(m_i^2/M_W^2), \quad (19)$$

where the loop function $X(x_i)$ can be found e.g. in Ref. [32].

As one can notice from Eq. (13), the scalar leptoquarks $S_{1,3}^{1/3}$ and vector leptoquarks $V_{2,3}^{1/3}$ and $U_3^{-1/3}$ give the following contribution to $b \rightarrow s\nu_j\bar{\nu}_i$:

$$C_R^{ij} = -\frac{1}{2\sqrt{2}G_F V_{tb} V_{ts}^*} \sum_{m,n=1}^3 V_{m3} V_{n2}^* \frac{g_{2L}^{mi} g_{2L}^{nj*}}{M_{V_2}^2}, \quad (20a)$$

$$\begin{aligned} C_L^{ij} &= -\frac{1}{2\sqrt{2}G_F V_{tb} V_{ts}^*} \sum_{m,n=1}^3 V_{m3} V_{n2}^* \\ &\times \left[\frac{g_{1L}^{mi} g_{1L}^{nj*}}{2M_{S_1}^2} + \frac{g_{3L}^{mi} g_{3L}^{nj*}}{2M_{S_3}^2} - \frac{2h_{3L}^{ni} h_{3L}^{mj*}}{M_{U_3}^2} \right]. \end{aligned} \quad (20b)$$

In the following, for simplicity we neglect the subleading $\mathcal{O}(\lambda)$ terms in Eq. (20) and keep only the $V_{tb} V_{cs}^* \simeq 1$ term.

One has to note that the $U_3^{-1/3}$ leptoquark does not affect $b \rightarrow c\ell\bar{\nu}$. In this way, as can be seen from Eq. (14), only the $g_{1(3)L}^{3l} g_{1(3)L}^{23*}$ couplings of the $S_{1(3)}^{1/3}$ leptoquarks can be constrained using both $b \rightarrow c\tau\bar{\nu}_l$ and $b \rightarrow s\nu_\tau\bar{\nu}_l$ processes. Nevertheless, assuming that the leptoquarks from the same $SU(2)$ triplet, namely, $U_3^{-1/3}$ and $U_3^{2/3}$, have masses of the same order, one can combine the constraints on $h_{3L}^{2l} h_{3L}^{33*}$.

Summing over all neutrino flavors and taking into account that the amplitudes with $i \neq j$ do not interfere with the SM contribution, the branching ratio can be written as

$$\begin{aligned} \frac{d\mathcal{B}(\bar{B} \rightarrow X_s \nu\bar{\nu})}{dx} &= \tau_B \frac{G_F^2}{12\pi^3} |V_{tb} V_{ts}^*|^2 m_b^5 S(x) \\ &\times \left[3C_L^{\text{SM}2} + \sum_{i,j=1}^3 (|C_L^{ij}|^2 + |C_R^{ij}|^2) \right. \\ &\left. + 2C_L^{\text{SM}} \sum_{i=1}^3 \mathcal{R}e[C_L^{i*}] \right], \end{aligned} \quad (21)$$

where $x = E_{\text{miss}}/m_b$ and the $S(x)$ function describes the shape of the missing energy spectrum [33]. In our estimation we set $m_s = 0$ (therefore $1/2 \leq x \leq 1$) and neglect the α_s and $1/m_b^2$ corrections.

Using the experimental limit on the inclusive branching ratio, determined by the ALEPH Collaboration [34],

$$\mathcal{B}^{\text{exp}}(B \rightarrow X_s \nu\bar{\nu}) < 6.4 \times 10^{-4} \quad \text{at the 90\% C.L.}, \quad (22)$$

and assuming for simplicity that only one specific ij combination of one type of leptoquarks contributes, we obtain constraints on the leptoquark couplings depicted in Fig. 1. In the case that the couplings are real, the obtained numbers are consistent with the result of Grossman *et al.* [33].

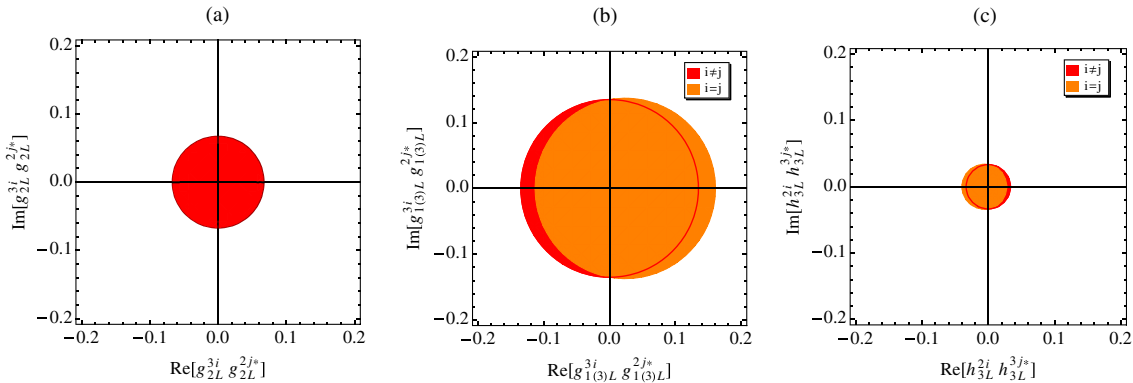


FIG. 1 (color online). Constraints on the leptoquark couplings contributing to the $b \rightarrow s\nu_j\bar{\nu}_i$ process using the experimental upper limit on $\mathcal{B}(B \rightarrow X_s \nu\bar{\nu})$.

C. Constraints from $\bar{B} \rightarrow D\tau\bar{\nu}$ and $\bar{B} \rightarrow D^*\tau\bar{\nu}$

Using the Wilson coefficients in Eq. (14), in Figs. 2–4 we provide constraints on various leptoquark effective couplings at the bottom quark mass scale and combine some of them with available bounds coming from $\mathcal{B}(\bar{B} \rightarrow X_s\nu\bar{\nu})$, discussed in the previous subsection. We consider the general case that the flavor of neutrino is arbitrary. The numerical results of two different sets of form factors are shown for comparison, including the theoretical uncertainties sketched in Appendix A.

In Fig. 2, as an example, we present the constraints on the $g_{1L}^{3l}g_{1L}^{23*}$ product of couplings of the $S_1^{1/3}$ leptoquark assuming that the other couplings are zero. The other constraints on $g_{3L}^{3l}g_{3L}^{23*}$ of the $S_3^{1/3}$ leptoquark and $h_{1(3)L}^{2l}h_{1(3)L}^{33*}$ of the $U_{1(3)}^{2/3}$ leptoquark can be easily obtained by rescaling and/or reflecting the constraints from $R(D^{(*)})$ in Fig. 2 [see Eq. (14a)].

Figures 2(c) and 2(d) represent the zoomed areas around the origin of the plots in Figs. 2(a) and 2(b),

respectively, combined with the constraints from Fig. 1(b). As one can notice, the case of $\bar{\nu}_l \neq \bar{\nu}_\tau$ is excluded since the constraints on $g_{1L}^{3l}g_{1L}^{23*}$ coming from $\bar{B} \rightarrow D^{(*)}\tau\bar{\nu}$ and $\bar{B} \rightarrow X_s\nu\bar{\nu}$ are inconsistent, namely, there is no overlap between red (disk) and green/yellow (centered annulus) allowed regions in Figs. 2(c) and 2(d). The results for the case of $\bar{\nu}_l = \bar{\nu}_\tau$ are consistent only at the 3σ level and force the couplings to be rather small. For other models, the similar conclusion can be made for $g_{3L}^{3l}g_{3L}^{23*}$ and $h_{3L}^{2l}h_{3L}^{33*}$. On the contrary, the $U_1^{2/3}$ leptoquark couplings, $h_{1L}^{2l}h_{1L}^{33*}$, remain unconstrained from $\bar{B} \rightarrow X_s\nu\bar{\nu}$ and the magnitude of the order of $O(1)$ can be sufficient to explain the current measurements of $R(D)$ and $R(D^*)$.

We find that the model with the vector $V_2^{1/3}$ leptoquark exchange with $g_{2L}^{3l}g_{2R}^{23*}$ couplings is hardly possible due to the low compatibility with the experimental data as can be seen from Fig. 3. We note that the allowed regions of 99% C.L. and 99.9% C.L. are shown in Fig. 3 since there is no allowed region even at 95% C.L. The $h_{1L}^{2l}h_{1R}^{33*}$ couplings of the $U_1^{2/3}$

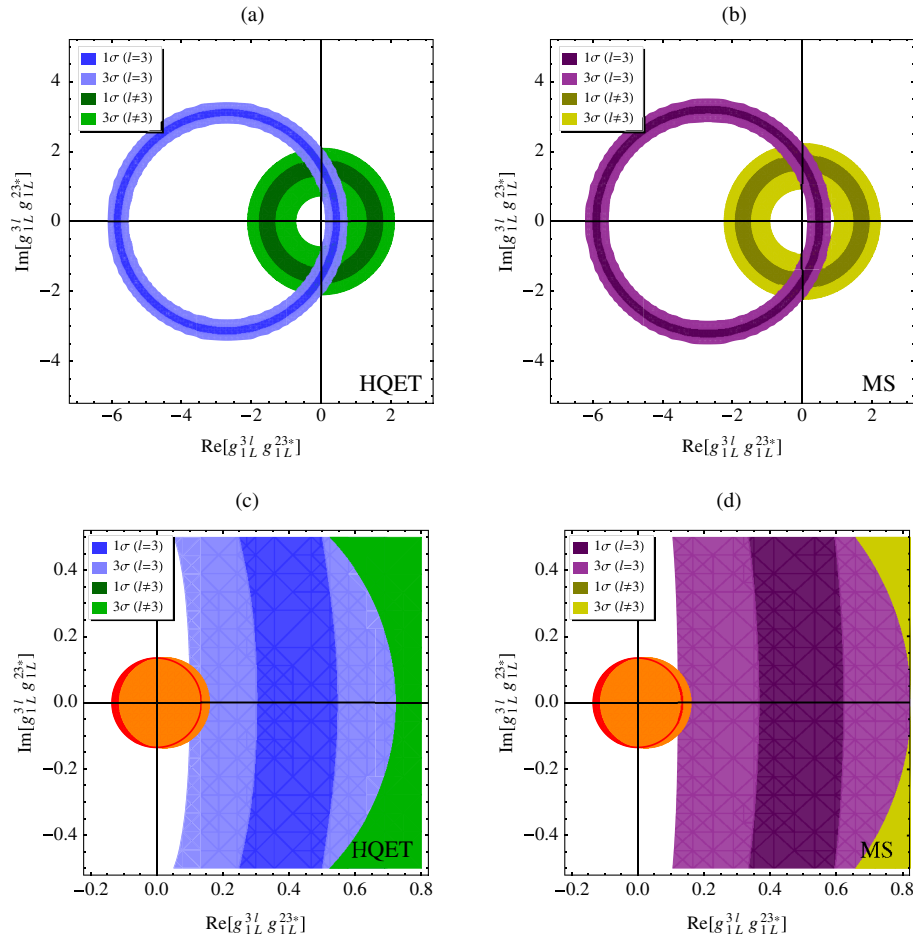


FIG. 2 (color online). Constraints on the leptoquark effective couplings at μ_b scale contributing to the C_{V_1} Wilson coefficient coming from the χ^2 fit of $R(D)$ and $R(D^*)$. The constraints are obtained by use of form factors evaluated in the HQET (a),(c) and the ones computed by Melikhov and Stech (b),(d). The zoomed areas around the origin of the plots in (a) and (b) are depicted in (c) and (d), respectively. The light gray (orange) and [dark gray (red)] circles show the constraints from the experimental upper limit on $\mathcal{B}(\bar{B} \rightarrow X_s\nu\bar{\nu}_l)$ for $l = \tau$ and $l \neq \tau$, respectively.

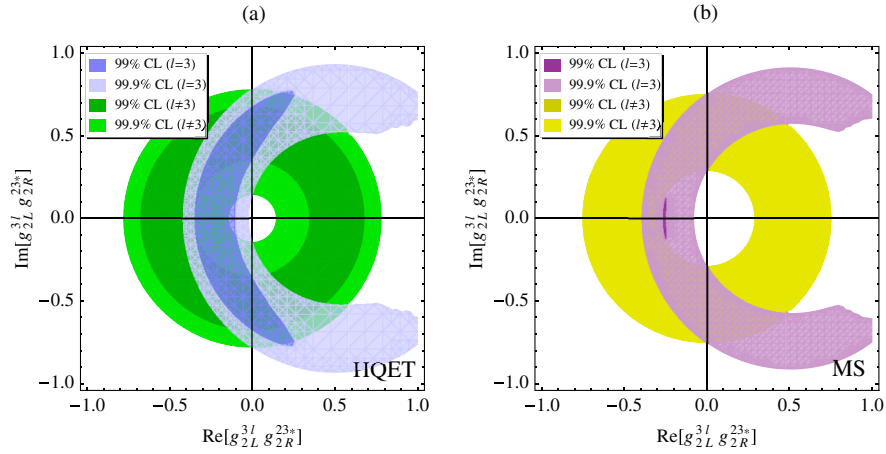


FIG. 3 (color online). Constraints on the leptoquark effective couplings at μ_b scale contributing to the C_{S_1} Wilson coefficient coming from the χ^2 fit of $R(D)$ and $R(D^*)$. The constraints presented in Figs. (a) and (b) are obtained by use of form factors evaluated in the HQET and the ones computed by Melikhov and Stech, respectively.

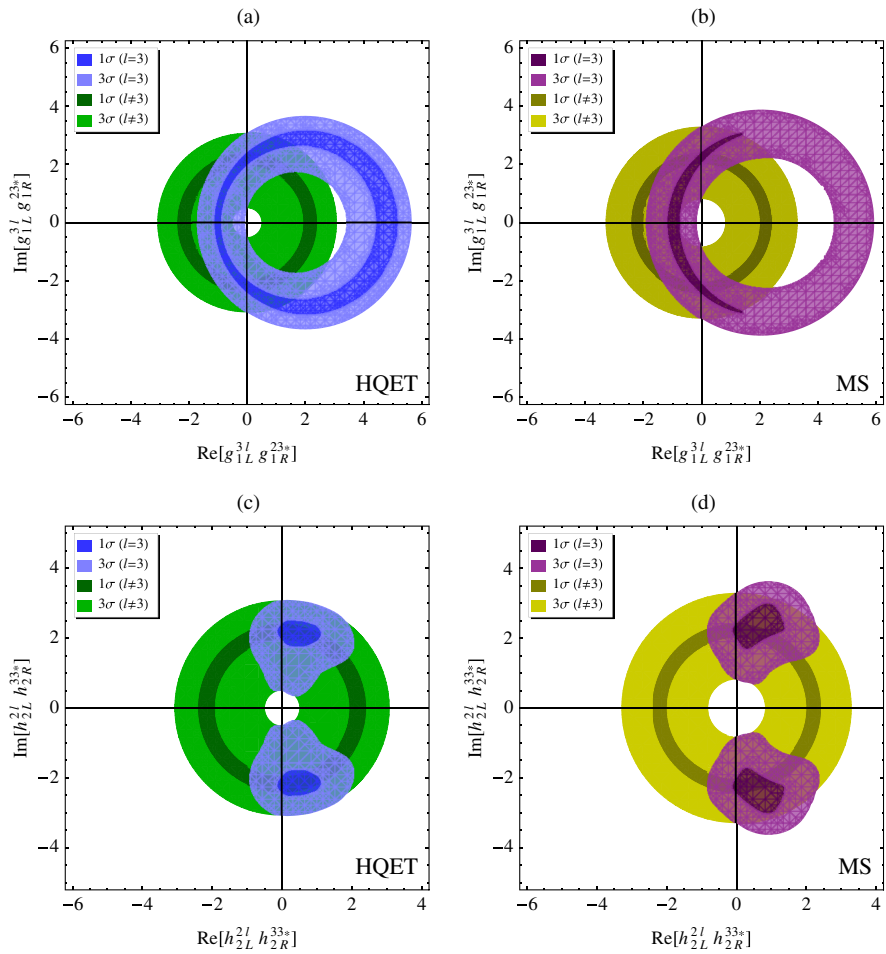


FIG. 4 (color online). Constraints on the leptoquark effective couplings at μ_b scale contributing to the C_{S_2} and C_T Wilson coefficients coming from the χ^2 fit of $R(D)$ and $R(D^*)$. The constraints presented in Figs. (a),(c) and (b),(d) are obtained by use of form factors evaluated in the HQET and the ones computed by Melikhov and Stech, respectively.

leptoquark have the same allowed space as $g_{2L}^{3l}g_{2R}^{23*}$ of the $V_2^{1/3}$ leptoquark in Fig. 3 [see Eq. (14c)].

In Fig. 4 we demonstrate that the scalar $S_1^{1/3}$ and $R_2^{2/3}$ leptoquark effective couplings, $g_{1L}^{3l}g_{1R}^{23*}$ and $h_{2L}^{2l}h_{2R}^{33*}$, of $O(1)$ are sufficient to explain the present data for the leptoquark mass scale of the order of 1 TeV. It is interesting to note from Figs. 4(c) and 4(d) that the $R_2^{2/3}$ leptoquark couplings are favored to be purely imaginary which could be tested directly by studying χ angular distribution in $\bar{B} \rightarrow D^*(\rightarrow D\pi)\tau\bar{\nu}$ (where χ is the azimuthal angle between the planes formed by the $W - \tau$ and $D^* - D$ systems in the \bar{B} rest frame).

D. Sensitivity of the constraints to hadronic form factors

To conclude this section, we discuss the sensitivity of the NP constraints to hadronic form factors and their theoretical uncertainties. In Figs. 2–4 we show the comparison of the resulting constraints on leptoquark effective couplings, obtained by using the form factors evaluated in the HQET by Caprini *et al.* [28] and the ones computed by Melikhov and Stech in the constituent quark model [29]. These two sets have fairly different uncertainties although both of them describe the experimental results of $\bar{B} \rightarrow D^{(*)}\ell\bar{\nu}$ and are consistent with the heavy quark symmetry.

We find that both sets of form factors give similar allowed regions in the parameter space for most leptoquark models. The constraints on the product of couplings of the scalar $S_{1(3)}^{1/3}$ and vector $U_{1(3)}^{2/3}$ leptoquarks with only left-handed couplings [$g_{1(3)L}^{3l}g_{1(3)L}^{23*}$ and $h_{1(3)L}^{2l}h_{1(3)L}^{33*}$, respectively] in Fig. 2 look practically identical and therefore the effect of the choice of the form factor set is negligible.

In our study we observe that in the case of the vector $V_2^{1/3}$ and $U_1^{2/3}$ leptoquarks with both left- and right-handed couplings ($g_{2L}^{3l}g_{2R}^{23*}$ and $h_{1L}^{2l}h_{1R}^{33*}$, respectively), the degree of exclusion highly depends on the employed form factors (see Fig. 3). One can notice from Fig. 3(b) that for the case of the MS form factors there is practically no allowed region at 99% C.L. which makes this model disfavored. This means that we must be careful about theoretical uncertainties when excluding NP models.

In Fig. 4 we show the resulting constraints on the scalar $S_1^{1/3}$ and $R_2^{2/3}$ leptoquark effective couplings ($g_{1L}^{3l}g_{1R}^{23*}$ and $h_{2L}^{2l}h_{2R}^{33*}$, respectively) which contribute to both C_{S_2} and C_T Wilson coefficients and therefore are sensitive to tensor form factors. One can notice that, compared to Fig. 2, the constraints in Fig. 4 look slightly different for two sets of form factors. The form factor uncertainty tends to cancel in the ratios $R(D^{(*)})$ for the case of the SM-like operators, $\mathcal{O}_{V_1}^l$, as can be seen in Fig. 2. On the other hand, we do not expect such cancellation in the case of the scalar and tensor operators, $\mathcal{O}_{S_{1,2}}^l$ and \mathcal{O}_T^l . This makes the NP constraints more sensitive to the tensor form factor uncertainties and

TABLE II. Comparison of the $\pm 1\sigma$ allowed ranges for the leptoquark effective couplings using the form factors evaluated in the HQET and the ones computed by Melikhov and Stech. The intervals for $g_{2L}^{33}g_{2R}^{23*}$ are given at 99% C.L. level due to the absence of the allowed space at 1σ and 2σ levels. The products of couplings are assumed to be purely real or imaginary.

	HQET	MS
$ Im[h_{2L}^{23}h_{2R}^{33*}] $	[1.92; 2.42]	[1.99; 2.44]
$Im[g_{1L}^{33}g_{1R}^{23*}]$		
$Re[g_{1L}^{33}g_{1R}^{23*}]$	[-1.12; -0.85] [4.40; 5.17]	[-1.16; -0.71]
$Re[h_{1L}^{23}h_{1L}^{33*}]$	[-2.97; -2.85] [0.15; 0.27]	[-3.01; -2.88] [0.18; 0.31]
$ Im[h_{1L}^{23}h_{1L}^{33*}] $	[0.65; 0.90]	[0.73; 0.97]
$Re[g_{2L}^{33}g_{2R}^{23*}]$	[-0.35; -0.10]	[-0.27; -0.24]
$Im[g_{2L}^{33}g_{2R}^{23*}]$	[0.34; 0.68]	

hence can explain the difference between the HQET and MS results in Fig. 4.

In Table II we give explicitly some numerical results for the allowed parameter space compatible with the experimental data at 1σ level (except for the vector $V_2^{1/3}$ leptoquark couplings $g_{2L}^{33}g_{2R}^{23*}$, for which we present the ranges at 99% C.L. due to the absence of the allowed space at 1σ and 2σ levels). For illustration, we assume the product of couplings to be purely real or purely imaginary. As one can see from Table II, the allowed ranges are well consistent for two sets of form factors. The exception is the $V_2^{1/3}$ leptoquark couplings $g_{2L}^{33}g_{2R}^{23*}$ which have a very tiny parameter space at 99% C.L. for the MS form factors.

Incidentally, we would like to note that the HQET parameters, ρ_{D,D^*}^2 and $R_{1,2}(1)$ (see Appendix A 3), are extracted from experiments by the *BABAR* and *Belle* collaborations [35–38] assuming only the SM contribution to the total amplitude of $\bar{B} \rightarrow D^{(*)}\ell\bar{\nu}_\ell$ ($\ell = e, \mu$). Therefore, in order to use the fitted HQET form factors, one has to make an important assumption that couplings of NP particles to light leptons are significantly suppressed as in the 2HDM-II and NP effects can be observed only in the taonic decay modes.

IV. CORRELATIONS BETWEEN OBSERVABLES

In order to distinguish between various NP models, we study the following observables which could be sensitive to NP:

- (i) τ forward-backward asymmetry,

$$\begin{aligned} \mathcal{A}_{\text{FB}} &= \frac{\int_0^1 \frac{d\Gamma}{d\cos\theta} d\cos\theta - \int_{-1}^0 \frac{d\Gamma}{d\cos\theta} d\cos\theta}{\int_{-1}^1 \frac{d\Gamma}{d\cos\theta} d\cos\theta} \\ &= \frac{\int b_\theta(q^2)dq^2}{\Gamma}, \end{aligned} \quad (23)$$

where θ is the angle between the three-momenta of τ and \bar{B} in the $\tau\bar{\nu}$ rest frame;

- (ii) τ polarization parameter by studying further τ decays,

$$P_\tau = \frac{\Gamma(\lambda_\tau = 1/2) - \Gamma(\lambda_\tau = -1/2)}{\Gamma(\lambda_\tau = 1/2) + \Gamma(\lambda_\tau = -1/2)}; \quad (24)$$

- (iii) D^* longitudinal polarization using the $D^* \rightarrow D\pi$ decay,

$$P_{D^*} = \frac{\Gamma(\lambda_{D^*} = 0)}{\Gamma(\lambda_{D^*} = 0) + \Gamma(\lambda_{D^*} = 1) + \Gamma(\lambda_{D^*} = -1)}. \quad (25)$$

Here, for brevity, Γ denotes $\Gamma(\bar{B} \rightarrow D^{(*)}\tau\bar{\nu})$. The q^2 distributions for various τ and D^* polarization states together with $b_\theta(q^2)$ can be found in Appendix B.

In order to determine θ angle, the τ momentum reconstruction is necessary. It is not apparent whether this is possible due to the two or more missing neutrinos in the decay modes under consideration [9]. Here we mention a proposal in LHCb to utilize the information on the vertices of \bar{B} and τ production/decay for identifying a $\bar{B} \rightarrow D^*\tau\bar{\nu}$ process in their environment [39,40]. The τ production/decay vertex information, which can be obtained using the $D^* \rightarrow D\pi/\tau \rightarrow 3h\nu$ decays, allows us to determine the three-momentum of τ in the lab frame with a two-fold ambiguity. Then, the same solution can be

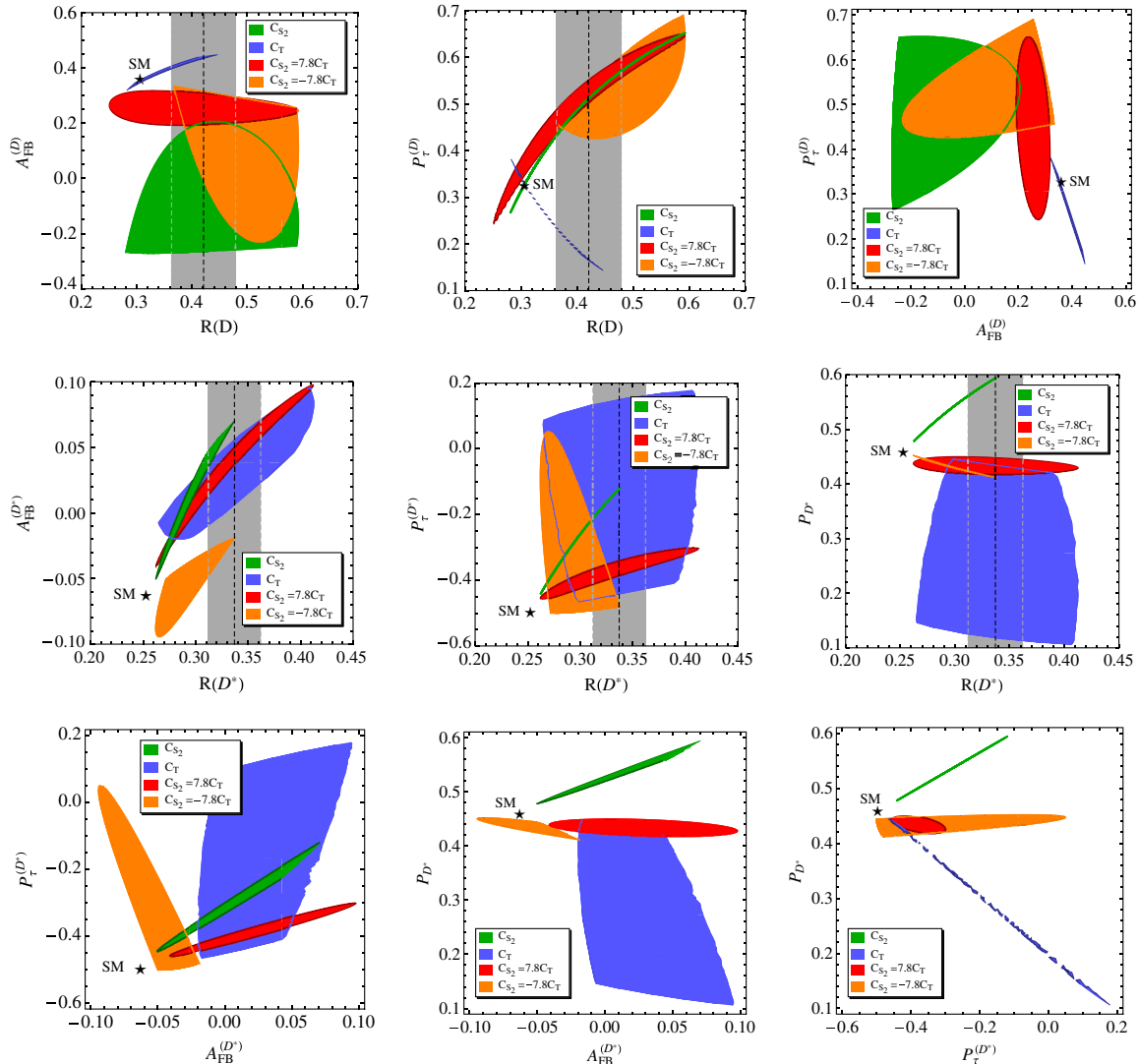


FIG. 5 (color online). The correlations between various observables [$R(D^{(*)})$, \mathcal{A}_{FB} , P_τ and P_{D^*}] for four different NP scenarios assuming $l = \tau$: the generic scalar [gray (green)] and tensor [black (blue)] contributions to the $C_{S_2}^\tau$ and C_T^τ Wilson coefficients, respectively; only $R_2^{2/3}$ [dark gray (red)] and $S_1^{1/3}$ [light gray (orange)] leptoquark contribution—the specific cases giving $C_{S_2}^\tau(\mu_b) = \pm 7.8C_T^\tau(\mu_b)$. The correlations were obtained by applying the constraints on the NP couplings from the χ^2 fit of $R(D)$ and $R(D^*)$ at 3σ level. The star corresponds to the SM prediction. The current experimental measurements of $R(D^{(*)})$ within $\pm 1\sigma$ range are shown in vertical bands.

applied for the \bar{B} meson case, knowing the \bar{B} production/decay vertices and the τ momentum. As a result, performing a boost to the $\tau\bar{\nu}$ rest frame, θ can be determined with a four-fold ambiguity. If a similar technique is available at super B factories, this ambiguity can be reduced to a two-fold one due to the full knowledge of the initial B meson kinematics.

The longitudinal τ polarization is measurable without reconstructing the τ momentum as is discussed in Ref. [12]. The expected precision at super B factories with 50 ab^{-1} is $\delta P_\tau \sim 0.04(0.03)$ for the $D^{(*)}$ mode. The D^* polarization is also measurable from the pion distribution in the D^* decay. The precision at super B factories with 50 ab^{-1} is estimated as $\delta P_{D^*} \sim 5 \times 10^{-3}$.

In Fig. 5 we present the correlations between various observables for four different scenarios assuming $l = \tau$ ¹:

- (1) the generic NP scalar contribution to $C_{S_2}^\tau$ [gray (green)];
- (2) the generic NP tensor contribution to C_T^τ [black (blue)];
- (3) the $R_2^{2/3}$ leptoquark contribution to $C_{S_2}^\tau$ and C_T^τ giving $C_{S_2}^\tau = 7.8C_T^\tau$ [dark gray (red)];
- (4) the $S_1^{1/3}$ leptoquark contribution to $C_{S_2}^\tau$ and C_T^τ giving $C_{S_2}^\tau = -7.8C_T^\tau$ [light gray (orange)].

The correlations are obtained by applying the constraints on the NP couplings from the χ^2 fit of $R(D)$ and $R(D^*)$ at 3σ level employing the central values of the HQET form factor parameters. The star corresponds to the SM prediction. The current experimental measurements of $R(D^{(*)})$ within $\pm 1\sigma$ interval are shown in vertical bands.

One can easily rewrite Eqs. (24) and (25) in the following forms:

$$\begin{aligned} (1 - P_\tau)\Gamma &= 2\Gamma(\lambda_\tau = -1/2), \\ (1 - P_{D^*})\Gamma &= \Gamma(\lambda_{D^*} = 1) + \Gamma(\lambda_{D^*} = -1). \end{aligned} \quad (26)$$

Then, we notice that the right-hand sides of Eq. (26) do not contain the scalar NP contribution [see Eqs. (A23)–(A25)]. Therefore, in the scenario 1, the correlations between P_τ/P_{D^*} and $R(D^{(*)})$ are uniquely determined.

As can be seen from Fig. 5, for some parameter spaces, one can clearly discriminate these four scenarios or at least exclude some of them. In particular, the longitudinal D^* polarization could be very useful to discriminate the models that have the generic scalar and tensor operators, $\mathcal{O}_{S_2}^\tau$ and \mathcal{O}_T^τ .

V. CONCLUSIONS

We have studied possible new physics explanations of the observed excess of $\bar{B} \rightarrow D^{(*)}\tau\bar{\nu}$ over the SM

¹Note that the contribution to $C_{V_1}^l$ of the $U_1^{2/3}$ leptoquark, whose effective couplings $h_{1L}^{2l}h_{1L}^{33*}$ remain unconstrained by $\mathcal{B}(\bar{B} \rightarrow X_s\nu\bar{\nu})$, gives the same asymmetry and polarizations as the SM.

predictions focusing on the leptoquark models. It has turned out that the $S_1^{1/3}$ scalar leptoquark with a nonvanishing product of couplings $g_{1L}^{3l}g_{1R}^{23*}$ and $R_2^{2/3}$ with $h_{2L}^{2l}h_{2R}^{33*}$ describe the present experimental data quite well. The required magnitudes of effective couplings are $O(1)$ for the leptoquark mass of 1 TeV. The interesting feature of these scenarios is that two favourable operators, namely, one of the scalar operators $\mathcal{O}_{S_2}^l$ and the tensor one \mathcal{O}_T^l , simultaneously appear and their Wilson coefficients are unambiguously related as $C_{S_2}^l = \mp 4C_T^l$ at the leptoquark mass scale.

Apart from the above two scenarios, the $U_1^{2/3}$ vector leptoquark with nonvanishing $h_{1L}^{2l}h_{1L}^{33*}$ that generates the $V - A$ operator $\mathcal{O}_{V_1}^l$ is also acceptable. The other scenarios in which $\mathcal{O}_{V_1}^l$ is induced, $S_{1(3)}^{1/3}$ with $g_{1(3)L}^{3l}g_{1(3)L}^{23*}$ and $U_3^{2/3}$ with $h_{3L}^{2l}h_{3L}^{33*}$, are hardly consistent because the experimental constraint from $B \rightarrow X_s\nu\bar{\nu}$ is mostly incompatible with those from $\bar{B} \rightarrow D^{(*)}\tau\bar{\nu}$. The scenarios that generate the scalar operator $\mathcal{O}_{S_1}^l$, $V_2^{1/3}$ with $g_{2L}^{3l}g_{2R}^{23*}$ and $U_1^{2/3}$ with $h_{1L}^{2l}h_{1R}^{33*}$, are disfavored as in the 2HDM-II.

Theoretical uncertainties in the hadronic form factors are carefully treated in our analysis. In particular, we have compared the results of two sets of the form factors, HQET and MS. These sets have rather different uncertainties although both of them describe the experimental results of $\bar{B} \rightarrow D^{(*)}\ell\bar{\nu}$ and are consistent with the heavy quark symmetry. We have shown that they give similar allowed regions in the parameter space of the leptoquark models in most cases. In some cases with small probabilities, however, the degree of exclusion highly depends on the employed form factors. This means that we must be deliberate about theoretical uncertainties in new physics contributions as well as the SM contributions in order to exclude models of new physics.

For further tests and discrimination of the allowed leptoquark models, we have examined correlations among the τ forward-backward asymmetries \mathcal{A}_{FB} , the τ polarizations P_τ , and the D^* longitudinal polarization P_{D^*} in some favorable cases. We have found that P_{D^*} is a sensitive observable to discriminate $\mathcal{O}_{S_2}^l$, \mathcal{O}_T^l and their mixture.

Measurements of these observables in addition to a more precise determination of $R(D^{(*)})$ are the key issues in order to identify the origin of the present excess of $\bar{B} \rightarrow D^{(*)}\tau\bar{\nu}$. LHCb and super B factories are capable of exploring new physics in this context together with the new particle search at LHC.

ACKNOWLEDGMENTS

This work is supported in part by the Japan Society for the Promotion of Science Grants-in-Aid for Scientific Research No. 20244037, No. 2540027 (M. T.), No. 2402804 (A. T.) and No. 248920 (R. W.).

APPENDIX A: HADRONIC MATRIX ELEMENTS**1. $\bar{B} \rightarrow D$**

The SM contribution is determined by the vector current operator and the relevant matrix element is written as

$$\begin{aligned} \langle D(k) | \bar{c} \gamma_\mu b | \bar{B}(p) \rangle &= \left[(p+k)_\mu - \frac{m_B^2 - m_D^2}{q^2} q_\mu \right] F_1(q^2) \\ &+ q_\mu \frac{m_B^2 - m_D^2}{q^2} F_0(q^2), \end{aligned} \quad (\text{A1})$$

where $F_1(0) = F_0(0)$ in order to cancel the divergence at $q^2 = 0$.

Using the equation of motion,

$$i \partial_\mu (\bar{c} \gamma^\mu b) = (m_b - m_c) \bar{c} b, \quad (\text{A2})$$

one can write the scalar operator matrix element as

$$\begin{aligned} \langle D(k) | \bar{c} b | \bar{B}(p) \rangle &= \frac{1}{m_b - m_c} q_\mu \langle D(k) | \bar{c} \gamma^\mu b | \bar{B}(p) \rangle \\ &= \frac{m_B^2 - m_D^2}{m_b - m_c} F_0(q^2). \end{aligned} \quad (\text{A3})$$

In our numerical analysis we use $m_b = (4.8 \pm 0.2)$ GeV and $m_c = (1.4 \pm 0.2)$ GeV [28,29] and treat the quark masses as a source of theoretical uncertainty.

The tensor² matrix element can be parametrized as

$$\langle D(k) | \bar{c} \sigma_{\mu\nu} b | \bar{B}(p) \rangle = -i(p_\mu k_\nu - k_\mu p_\nu) \frac{2F_T(q^2)}{m_B + m_D}. \quad (\text{A4})$$

Comparing the respective matrix elements in Eqs. (A1), (A4), (A14), and (A20), one finds the following relations between the $F_{1,0,T}$ and $h_{\pm,T}$ form factors, usually used in the HQET (for the HQET parametrization see Appendix A 3):

$$\begin{aligned} F_1(q^2) &= \frac{1}{2\sqrt{m_B m_D}} [(m_B + m_D) h_+(w(q^2)) \\ &- (m_B - m_D) h_-(w(q^2))], \\ F_0(q^2) &= \frac{1}{2\sqrt{m_B m_D}} \left[\frac{(m_B + m_D)^2 - q^2}{m_B + m_D} h_+(w(q^2)) \right. \\ &\left. - \frac{(m_B - m_D)^2 - q^2}{m_B - m_D} h_-(w(q^2)) \right], \\ F_T(q^2) &= \frac{m_B + m_D}{2\sqrt{m_B m_D}} h_T(w(q^2)). \end{aligned} \quad (\text{A5})$$

2. $\bar{B} \rightarrow D^*$

The vector and axial vector operator matrix elements can be written as

$$\begin{aligned} \langle D^*(k, \varepsilon) | \bar{c} \gamma_\mu b | \bar{B}(p) \rangle &= -i \epsilon_{\mu\nu\rho\sigma} \varepsilon^{\nu*} p^\rho k^\sigma \frac{2V(q^2)}{m_B + m_{D^*}}, \\ \langle D^*(k, \varepsilon) | \bar{c} \gamma_\mu \gamma_5 b | \bar{B}(p) \rangle &= \varepsilon^{\mu*} (m_B + m_{D^*}) A_1(q^2) - (p+k)_\mu (\varepsilon^* q) \frac{A_2(q^2)}{m_B + m_{D^*}} \\ &- q_\mu (\varepsilon^* q) \frac{2m_{D^*}}{q^2} [A_3(q^2) - A_0(q^2)], \end{aligned} \quad (\text{A6})$$

where

$$A_3(q^2) = \frac{m_B + m_{D^*}}{2m_{D^*}} A_1(q^2) - \frac{m_B - m_{D^*}}{2m_{D^*}} A_2(q^2), \quad (\text{A7})$$

with $A_3(0) = A_0(0)$.

The pseudoscalar matrix element can be determined by using the equation of motion,

$$i \partial_\mu (\bar{c} \gamma^\mu \gamma_5 b) = -(m_b + m_c) \bar{c} \gamma_5 b, \quad (\text{A8})$$

and is given by

$$\langle D^*(k, \varepsilon) | \bar{c} \gamma_5 b | \bar{B}(p) \rangle = -\frac{1}{m_b + m_c} q_\mu \langle D^*(k, \varepsilon) | \bar{c} \gamma^\mu \gamma_5 b | \bar{B}(p) \rangle = -(\varepsilon^* q) \frac{2m_{D^*}}{m_b + m_c} A_0(q^2). \quad (\text{A9})$$

The tensor operator contribution can be parametrized as

$$\begin{aligned} \langle D^*(k, \varepsilon) | \bar{c} \sigma_{\mu\nu} b | \bar{B}(p) \rangle &= \epsilon_{\mu\nu\rho\sigma} \left\{ -\varepsilon^{*\rho} (p+k)^\sigma T_1(q^2) + \varepsilon^{*\rho} q^\sigma \frac{m_B^2 - m_{D^*}^2}{q^2} [T_1(q^2) - T_2(q^2)] \right. \\ &\left. + 2 \frac{(\varepsilon^* \cdot q)}{q^2} p^\rho k^\sigma \left[T_1(q^2) - T_2(q^2) - \frac{q^2}{m_B^2 - m_{D^*}^2} T_3(q^2) \right] \right\}, \end{aligned} \quad (\text{A10})$$

where the T_i form factors, commonly used in semileptonic B decays, are usually determined as

²Pseudotensor matrix element can be evaluated using the relation $\bar{c} \sigma_{\mu\nu} \gamma_5 b = -\frac{i}{2} \epsilon_{\mu\nu\alpha\beta} \bar{c} \sigma^{\alpha\beta} b$. In this work we use the convention $\epsilon^{0123} = -1$.

$$\begin{aligned} \langle D^*(k, \varepsilon) | \bar{c} \sigma_{\mu\nu} q^\nu b | \bar{B}(p) \rangle &= \epsilon_{\mu\nu\rho\sigma} \varepsilon^{*\nu} p^\rho k^\sigma 2T_1(q^2), \\ \langle D^*(k, \varepsilon) | \bar{c} \sigma_{\mu\nu} \gamma_5 q^\nu b | \bar{B}(p) \rangle &= -[(m_B^2 - m_{D^*}^2) \varepsilon^{*\mu} - (\varepsilon^* q)(p+k)_\mu] T_2(q^2) - (\varepsilon^* q) \left[q_\mu - \frac{q^2}{m_B^2 - m_{D^*}^2} (p+k)_\mu \right] T_3(q^2). \end{aligned} \quad (\text{A11})$$

Analogously, matching Eqs. (A6) and (A10) to Eqs. (A14) and (A20), the form factors V , A_i and T_i can be related to h_V , h_{A_i} , and h_{T_i} as follows:

$$\begin{aligned} V(q^2) &= \frac{m_B + m_{D^*}}{2\sqrt{m_B m_{D^*}}} h_V(w(q^2)), \quad A_1(q^2) = \frac{(m_B + m_{D^*})^2 - q^2}{2\sqrt{m_B m_{D^*}}(m_B + m_{D^*})} h_{A_1}(w(q^2)), \\ A_2(q^2) &= \frac{m_B + m_{D^*}}{2\sqrt{m_B m_{D^*}}} \left[h_{A_3}(w(q^2)) + \frac{m_{D^*}}{m_B} h_{A_2}(w(q^2)) \right], \end{aligned} \quad (\text{A12})$$

$$\begin{aligned} A_0(q^2) &= \frac{1}{2\sqrt{m_B m_{D^*}}} \left[\frac{(m_B + m_{D^*})^2 - q^2}{2m_{D^*}} h_{A_1}(w(q^2)) - \frac{m_B^2 - m_{D^*}^2 + q^2}{2m_B} h_{A_2}(w(q^2)) - \frac{m_B^2 - m_{D^*}^2 - q^2}{2m_{D^*}} h_{A_3}(w(q^2)) \right], \\ T_1(q^2) &= \frac{1}{2\sqrt{m_B m_{D^*}}} [(m_B + m_{D^*}) h_{T_1}(w(q^2)) - (m_B - m_{D^*}) h_{T_2}(w(q^2))], \\ T_2(q^2) &= \frac{1}{2\sqrt{m_B m_{D^*}}} \left[\frac{(m_B + m_{D^*})^2 - q^2}{m_B + m_{D^*}} h_{T_1}(w(q^2)) - \frac{(m_B - m_{D^*})^2 - q^2}{m_B - m_{D^*}} h_{T_2}(w(q^2)) \right], \\ T_3(q^2) &= \frac{1}{2\sqrt{m_B m_{D^*}}} \left[(m_B - m_{D^*}) h_{T_1}(w(q^2)) - (m_B + m_{D^*}) h_{T_2}(w(q^2)) - 2 \frac{m_B^2 - m_{D^*}^2}{m_B} h_{T_3}(w(q^2)) \right]. \end{aligned} \quad (\text{A13})$$

3. HQET form factors

We define the form factors of the vector and axial vector operators as

$$\langle D(v') | \bar{c} \gamma_\mu b | \bar{B}(v) \rangle = \sqrt{m_B m_{D^*}} [h_+(w)(v + v')_\mu + h_-(w)(v - v')_\mu], \quad (\text{A14a})$$

$$\langle D^*(v', \varepsilon) | \bar{c} \gamma_\mu b | \bar{B}(v) \rangle = i\sqrt{m_B m_{D^*}} h_V(w) \epsilon_{\mu\nu\rho\sigma} \varepsilon^{*\nu} v'^\rho v^\sigma,$$

$$\langle D^*(v', \varepsilon) | \bar{c} \gamma_\mu \gamma_5 b | \bar{B}(v) \rangle = \sqrt{m_B m_{D^*}} [h_{A_1}(w)(w+1) \varepsilon_\mu^* - (\varepsilon^* \cdot v)(h_{A_2}(w)v_\mu + h_{A_3}(w)v'_\mu)], \quad (\text{A14b})$$

where $v = p_B/m_B$, $v' = k/m_{D^*}$ and $w(q^2) = v \cdot v' = (m_B^2 + m_{D^*}^2 - q^2)/2m_B m_{D^*}$.

In turn, using the parametrization of Caprini *et al.* [28], the HQET form factors can be expressed as

$$\begin{aligned} h_+(w) &= \frac{1}{2(1 + r_D^2 - 2r_D w)} [-(1 + r_D)^2(w-1)V_1(w) + (1 - r_D)^2(w+1)S_1(w)], \\ h_-(w) &= \frac{(1 - r_D^2)(w+1)}{2(1 + r_D^2 - 2r_D w)} [S_1(w) - V_1(w)], \end{aligned} \quad (\text{A15a})$$

$$h_V(w) = R_1(w)h_{A_1}(w), \quad h_{A_2}(w) = \frac{R_2(w) - R_3(w)}{2r_{D^*}} h_{A_1}(w), \quad h_{A_3}(w) = \frac{R_2(w) + R_3(w)}{2} h_{A_1}(w), \quad (\text{A15b})$$

where $r_{D^{(*)}} = m_{D^{(*)}}/m_B$. The w dependencies are parametrized as [28]

$$\begin{aligned} V_1(w) &= V_1(1)[1 - 8\rho_D^2 z + (51\rho_D^2 - 10)z^2 - (252\rho_D^2 - 84)z^3], \\ h_{A_1}(w) &= h_{A_1}(1)[1 - 8\rho_{D^*}^2 z + (53\rho_{D^*}^2 - 15)z^2 - (231\rho_{D^*}^2 - 91)z^3], \\ R_1(w) &= R_1(1) - 0.12(w-1) + 0.05(w-1)^2, \quad R_2(w) = R_2(1) + 0.11(w-1) - 0.06(w-1)^2, \\ R_3(w) &= 1.22 - 0.052(w-1) + 0.026(w-1)^2, \end{aligned} \quad (\text{A16})$$

where $z(w) = (\sqrt{w+1} - \sqrt{2})/(\sqrt{w+1} + \sqrt{2})$. The $S_1(w)$ form factor is taken from Ref. [12],

$$S_1(w) = V_1(w)[1 + \Delta(-0.019 + 0.041(w-1) - 0.015(w-1)^2)], \quad (\text{A17})$$

with $\Delta = 1 \pm 1$.

The fitted parameters, determined by the HFAG, are [41]

$$\rho_D^2 = 1.186 \pm 0.054, \quad \rho_{D^*}^2 = 1.207 \pm 0.026, \quad R_1(1) = 1.403 \pm 0.033, \quad R_2(1) = 0.854 \pm 0.020. \quad (\text{A18})$$

Although the form factor normalizations, $V_1(1)$ and $h_{A_1}(1)$, vanish in the $R(D)$ and $R(D^*)$ ratios, for completeness we provide below the latest lattice QCD calculations from Refs. [42,43], respectively,

$$V_1(1) = 1.074 \pm 0.024, \quad h_{A_1}(1) = 0.908 \pm 0.017. \quad (\text{A19})$$

The matrix elements of the tensor operator can be expressed in the following way [24]:

$$\langle D(v') | \bar{c} \sigma_{\mu\nu} b | \bar{B}(v) \rangle = -i \sqrt{m_B m_D} h_T(w) [v_\mu v'_\nu - v_\nu v'_\mu], \quad (\text{A20a})$$

$$\begin{aligned} \langle D^*(v', \varepsilon) | \bar{c} \sigma_{\mu\nu} b | \bar{B}(v) \rangle &= -\sqrt{m_B m_{D^*}} \epsilon_{\mu\nu\rho\sigma} [h_{T_1}(w) \varepsilon^{*\rho} (v + v')^\sigma + h_{T_2}(w) \varepsilon^{*\rho} (v - v')^\sigma \\ &\quad + h_{T_3}(w) (\varepsilon^* \cdot v) (v + v')^\rho (v - v')^\sigma]. \end{aligned} \quad (\text{A20b})$$

As in the case of scalar operators, the equation of motion,

$$\partial_\mu (\bar{c} \sigma^{\mu\nu} b) = -(m_b + m_c) \bar{c} \gamma^\nu b - (i \partial^\nu c) b + \bar{c} (i \partial^\nu b), \quad (\text{A21})$$

gives us the following relations between the tensor and vector form factors:

$$h_T(w) = \frac{m_b + m_c}{m_B + m_D} \left[h_+(w) - \frac{1 + r_D}{1 - r_D} h_-(w) \right], \quad (\text{A22a})$$

$$h_{T_1}(w) = \frac{1}{2(1 + r_{D^*}^2 - 2r_{D^*} w)} \left[\frac{m_b - m_c}{m_B - m_{D^*}} (1 - r_{D^*})^2 (w + 1) h_{A_1}(w) - \frac{m_b + m_c}{m_B + m_{D^*}} (1 + r_{D^*})^2 (w - 1) h_V(w) \right],$$

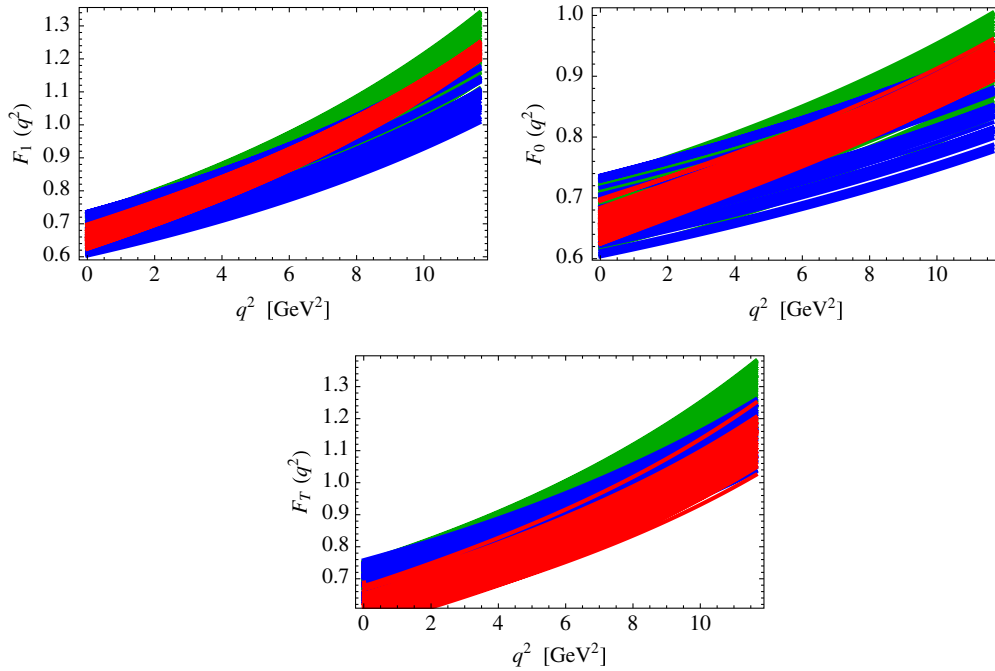


FIG. 6 (color online). The $\bar{B} \rightarrow D$ form factors evaluated in the HQET [dark gray (red)], calculated by Melikhov and Stech [29] [black (blue)] and by Cheng *et al.* [44] [gray (green)]. The calculation of the scalar and tensor form factors is absent in Ref. [44], therefore the equations of motion in the quark currents are used in order to express it in terms of $F_{1,0}(q^2)$.

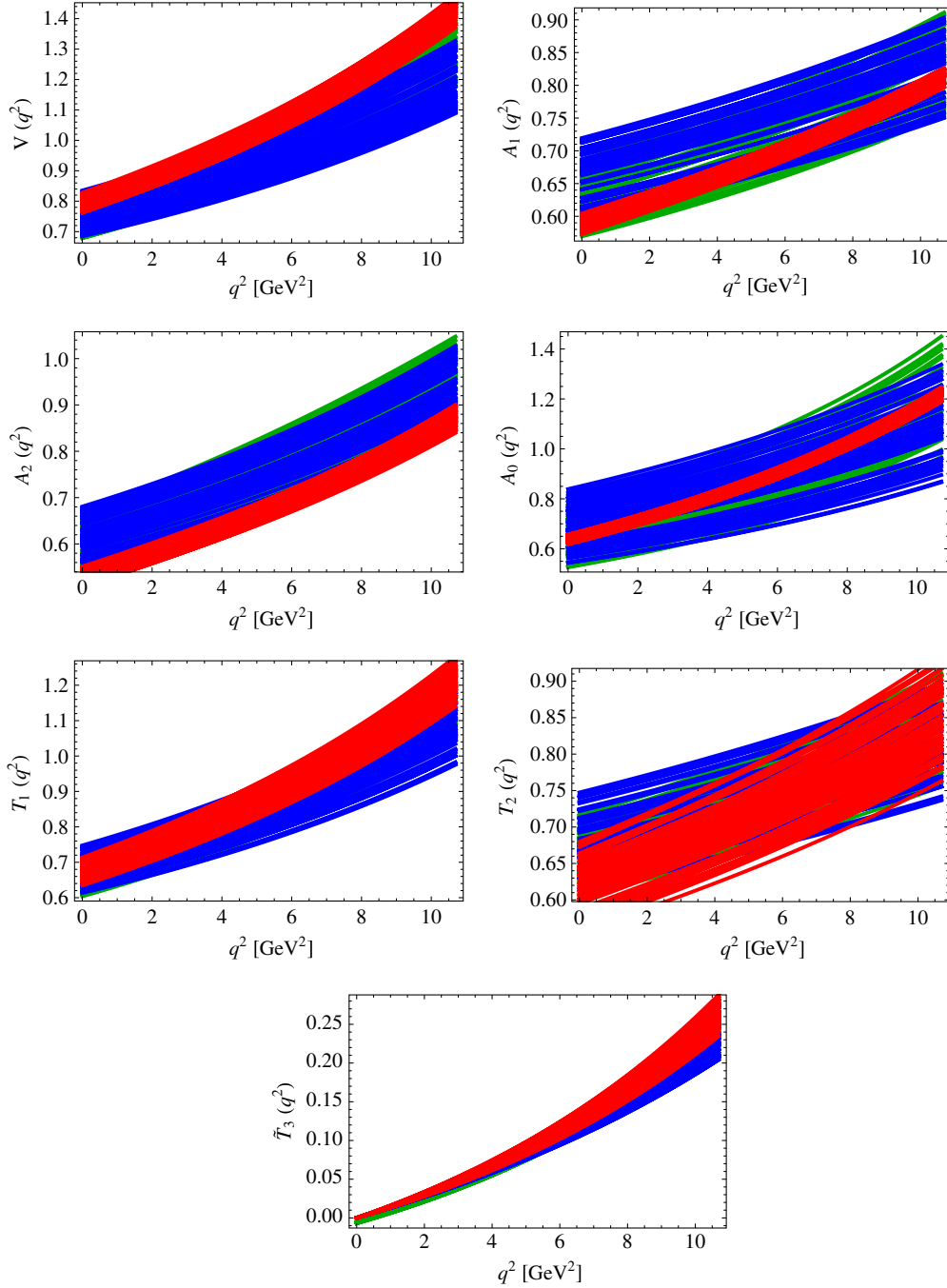


FIG. 7 (color online). The $\bar{B} \rightarrow D^*$ form factors evaluated in HQET [dark gray (red)], calculated by Melikhov and Stech [29] [black (blue)] and by Cheng *et al.* [44] [gray (green)]. The calculation of the scalar and tensor form factors is absent in Ref. [44]; therefore, we used the equations of motion in the quark currents in order to express $T_{1,2,3}(q^2)$ in terms of vector and axial vector form factors, $V(q^2)$ and $A_{0,1,2}(q^2)$. Here $\tilde{T}_3(q^2)$ is defined as $\tilde{T}_3(q^2) = T_3(q^2)q^2/(m_B^2 - m_{D^*}^2)$.

$$\begin{aligned}
 h_{T_2}(w) &= \frac{(1 - r_{D^*}^2)(w + 1)}{2(1 + r_{D^*}^2 - 2r_{D^*}w)} \left[\frac{m_b - m_c}{m_B - m_{D^*}} h_{A_1}(w) - \frac{m_b + m_c}{m_B + m_{D^*}} h_V(w) \right], \\
 h_{T_3}(w) &= -\frac{1}{2(1 + r_{D^*}^2)(1 + r_{D^*}^2 - 2r_{D^*}w)} \left[2 \frac{m_b - m_c}{m_B - m_{D^*}} r_{D^*}(w + 1) h_{A_1}(w) + \frac{m_b - m_c}{m_B - m_{D^*}} (1 + r_{D^*}^2 - 2r_{D^*}w) \right. \\
 &\quad \left. \times (h_{A_3}(w) - r_{D^*} h_{A_2}(w)) - \frac{m_b + m_c}{m_B + m_{D^*}} (1 + r_{D^*}^2)^2 h_V(w) \right], \tag{A22b}
 \end{aligned}$$

where the residual momenta of $O(\Lambda_{\text{QCD}})$ are neglected.

4. Comparison of the form factors

Here we compare three sets of form factors, evaluated in the HQET, computed by Melikhov and Stech [29], and Cheng *et al.* [44]. Theoretical uncertainties are not quoted directly in Refs. [29,44]; however, from the fine agreement obtained in the cases where the checks are possible, the authors of Ref. [29] believe that the accuracy of their predictions do not exceed 10%. Therefore, to be conservative, we vary the values of the form factors at $q^2 = 0$ within $\pm 10\%$ around their central values. As for the HQET form factors, all theoretical parameters are supposed to have flat distributions and are randomly varied within a $\pm 1\sigma$ region.

The heavy quark limit behavior is examined in Refs. [29,44] and the requirement of the heavy quark symmetry is satisfied. Therefore, as can be seen from Figs. 6 and 7, there is a reasonable agreement among these three sets.

APPENDIX B: DISTRIBUTIONS AND POLARIZATIONS

The q^2 distributions for a given polarization of τ are as follows:

$$\begin{aligned} \frac{d\Gamma^{\lambda_\tau=1/2}(\bar{B} \rightarrow D\tau\bar{\nu}_l)}{dq^2} &= \frac{G_F^2 |V_{cb}|^2}{192\pi^3 m_B^3} q^2 \sqrt{\lambda_D(q^2)} \left(1 - \frac{m_\tau^2}{q^2}\right)^2 \\ &\times \left\{ \frac{1}{2} |\delta_{l\tau} + C_{V_1}^l + C_{V_2}^l|^2 \frac{m_\tau^2}{q^2} (H_{V,0}^{s2} + 3H_{V,i}^{s2}) + \frac{3}{2} |C_{S_1}^l + C_{S_2}^l|^2 H_S^2 + 8|C_T^l|^2 H_T^2 \right. \\ &\left. + 3\mathcal{R}e[(\delta_{l\tau} + C_{V_1}^l + C_{V_2}^l)(C_{S_1}^{l*} + C_{S_2}^{l*})] \frac{m_\tau}{\sqrt{q^2}} H_S^s H_{V,i}^s - 4\mathcal{R}e[(\delta_{l\tau} + C_{V_1}^l + C_{V_2}^l)C_T^{l*}] \frac{m_\tau}{\sqrt{q^2}} H_T^s H_{V,0}^s \right\}, \end{aligned} \quad (\text{A23a})$$

$$\begin{aligned} \frac{d\Gamma^{\lambda_\tau=-1/2}(\bar{B} \rightarrow D\tau\bar{\nu}_l)}{dq^2} &= \frac{G_F^2 |V_{cb}|^2}{192\pi^3 m_B^3} q^2 \sqrt{\lambda_D(q^2)} \left(1 - \frac{m_\tau^2}{q^2}\right)^2 \\ &\times \left\{ |\delta_{l\tau} + C_{V_1}^l + C_{V_2}^l|^2 H_{V,0}^{s2} + 16|C_T^l|^2 \frac{m_\tau^2}{q^2} H_T^2 - 8\mathcal{R}e[(\delta_{l\tau} + C_{V_1}^l + C_{V_2}^l)C_T^{l*}] \frac{m_\tau}{\sqrt{q^2}} H_T^s H_{V,0}^s \right\}, \end{aligned} \quad (\text{A23b})$$

$$\begin{aligned} \frac{d\Gamma^{\lambda_\tau=1/2}(\bar{B} \rightarrow D^*\tau\bar{\nu}_l)}{dq^2} &= \frac{G_F^2 |V_{cb}|^2}{192\pi^3 m_B^3} q^2 \sqrt{\lambda_{D^*}(q^2)} \left(1 - \frac{m_\tau^2}{q^2}\right)^2 \times \left\{ \frac{1}{2} (|\delta_{l\tau} + C_{V_1}^l|^2 + |C_{V_2}^l|^2) \frac{m_\tau^2}{q^2} (H_{V,+}^2 + H_{V,-}^2 + H_{V,0}^2 + 3H_{V,i}^2) \right. \\ &- \mathcal{R}e[(\delta_{l\tau} + C_{V_1}^l)C_{V_2}^{l*}] \frac{m_\tau^2}{q^2} (H_{V,0}^2 + 2H_{V,+}H_{V,-} + 3H_{V,i}^2) + \frac{3}{2} |C_{S_1}^l \\ &- C_{S_2}^l|^2 H_S^2 + 8|C_T^l|^2 (H_{T,+}^2 + H_{T,-}^2 + H_{T,0}^2) + 3\mathcal{R}e[(\delta_{l\tau} + C_{V_1}^l - C_{V_2}^l)(C_{S_1}^{l*} - C_{S_2}^{l*})] \\ &\times \frac{m_\tau}{\sqrt{q^2}} H_S H_{V,i} - 4\mathcal{R}e[(\delta_{l\tau} + C_{V_1}^l)C_T^{l*}] \frac{m_\tau}{\sqrt{q^2}} (H_{T,0}H_{V,0} + H_{T,+}H_{V,+} - H_{T,-}H_{V,-}) \\ &\left. + 4\mathcal{R}e[C_{V_2}^l C_T^{l*}] \frac{m_\tau}{\sqrt{q^2}} (H_{T,0}H_{V,0} + H_{T,+}H_{V,-} - H_{T,-}H_{V,+}) \right\}, \end{aligned} \quad (\text{A24a})$$

$$\begin{aligned} \frac{d\Gamma^{\lambda_\tau=-1/2}(\bar{B} \rightarrow D^*\tau\bar{\nu}_l)}{dq^2} &= \frac{G_F^2 |V_{cb}|^2}{192\pi^3 m_B^3} q^2 \sqrt{\lambda_{D^*}(q^2)} \left(1 - \frac{m_\tau^2}{q^2}\right)^2 \times \left\{ (|\delta_{l\tau} + C_{V_1}^l|^2 + |C_{V_2}^l|^2) (H_{V,+}^2 + H_{V,-}^2 + H_{V,0}^2) \right. \\ &- 2\mathcal{R}e[(\delta_{l\tau} + C_{V_1}^l)C_{V_2}^{l*}] (H_{V,0}^2 + 2H_{V,+}H_{V,-}) + 16|C_T^l|^2 \frac{m_\tau^2}{q^2} (H_{T,+}^2 + H_{T,-}^2 + H_{T,0}^2) \\ &- 8\mathcal{R}e[(\delta_{l\tau} + C_{V_1}^l)C_T^{l*}] \frac{m_\tau}{\sqrt{q^2}} (H_{T,0}H_{V,0} + H_{T,+}H_{V,+} - H_{T,-}H_{V,-}) \\ &\left. + 8\mathcal{R}e[C_{V_2}^l C_T^{l*}] \frac{m_\tau}{\sqrt{q^2}} (H_{T,0}H_{V,0} + H_{T,+}H_{V,-} - H_{T,-}H_{V,+}) \right\}. \end{aligned} \quad (\text{A24b})$$

For the fixed polarization of D^* , the distributions are given by

$$\begin{aligned}
\frac{d\Gamma^{\lambda_{D^*}=\pm 1}(\bar{B} \rightarrow D^* \tau \bar{\nu}_l)}{dq^2} &= \frac{G_F^2 |V_{cb}|^2}{192\pi^3 m_B^3} q^2 \sqrt{\lambda_{D^*}(q^2)} \left(1 - \frac{m_\tau^2}{q^2}\right)^2 \\
&\times \left\{ \left(1 + \frac{m_\tau^2}{2q^2}\right) (|\delta_{l\tau} + C_{V_1}^l|^2 H_{V,\pm}^2 + |C_{V_2}^l|^2 H_{V,\mp}^2 - 2\mathcal{R}e[(\delta_{l\tau} + C_{V_1}^l) C_{V_2}^{l*}] H_{V,+} H_{V,-}) \right. \\
&+ 8|C_T^l|^2 \left(1 + \frac{2m_\tau^2}{q^2}\right) H_{T,\pm}^2 \mp 12\mathcal{R}e[(\delta_{l\tau} + C_{V_1}^l) C_T^{l*}] \frac{m_\tau}{\sqrt{q^2}} H_{T,\pm} H_{V,\pm} \pm 12\mathcal{R}e[C_{V_2}^l C_T^{l*}] \frac{m_\tau}{\sqrt{q^2}} H_{T,\pm} H_{V,\mp} \left. \right\},
\end{aligned} \tag{A25a}$$

$$\begin{aligned}
\frac{d\Gamma^{\lambda_{D^*}=0}(\bar{B} \rightarrow D^* \tau \bar{\nu}_l)}{dq^2} &= \frac{G_F^2 |V_{cb}|^2}{192\pi^3 m_B^3} q^2 \sqrt{\lambda_{D^*}(q^2)} \left(1 - \frac{m_\tau^2}{q^2}\right)^2 \\
&\times \left\{ |\delta_{l\tau} + C_{V_1}^l - C_{V_2}^l|^2 \left[\left(1 + \frac{m_\tau^2}{2q^2}\right) H_{V,0}^2 + \frac{3m_\tau^2}{2q^2} H_{V,t}^2 \right] \right. \\
&+ \frac{3}{2} |C_{S_1}^l - C_{S_2}^l|^2 H_S^2 + 8|C_T^l|^2 \left(1 + \frac{2m_\tau^2}{q^2}\right) H_{T,0}^2 + 3\mathcal{R}e[(\delta_{l\tau} + C_{V_1}^l - C_{V_2}^l)(C_{S_1}^{l*} - C_{S_2}^{l*})] \frac{m_\tau}{\sqrt{q^2}} H_S H_{V,t} \\
&\left. - 12\mathcal{R}e[(\delta_{l\tau} + C_{V_1}^l - C_{V_2}^l) C_T^{l*}] \frac{m_\tau}{\sqrt{q^2}} H_{T,0} H_{V,0} \right\}.
\end{aligned} \tag{A25b}$$

We note that the distributions for $\lambda_\tau = -1/2$ and $\lambda_{D^*} = \pm 1$ do not contain $C_{S_{1,2}}^l$ which makes them totally insensitive to the NP scalar operators.

Writing the angular distribution as

$$\frac{d^2\Gamma}{dq^2 d\cos\theta} = a_\theta(q^2) + b_\theta(q^2) \cos\theta + c_\theta(q^2) \cos^2\theta, \tag{A26}$$

the angular coefficient b_θ , which determines the lepton forward-backward asymmetry, is given by

$$\begin{aligned}
b_\theta^{(D)}(q^2) &= \frac{G_F^2 |V_{cb}|^2}{128\pi^3 m_B^3} q^2 \sqrt{\lambda_D(q^2)} \left(1 - \frac{m_\tau^2}{q^2}\right)^2 \\
&\times \left\{ |\delta_{l\tau} + C_{V_1}^l + C_{V_2}^l|^2 \frac{m_\tau^2}{q^2} H_{V,0}^s H_{V,t}^s + \mathcal{R}e[(\delta_{l\tau} + C_{V_1}^l + C_{V_2}^l)(C_{S_1}^{l*} + C_{S_2}^{l*})] \frac{m_\tau}{\sqrt{q^2}} H_S^s H_{V,0}^s \right. \\
&\left. - 4\mathcal{R}e[(\delta_{l\tau} + C_{V_1}^l + C_{V_2}^l) C_T^{l*}] \frac{m_\tau}{\sqrt{q^2}} H_T^s H_{V,t}^s - 4\mathcal{R}e[(C_{S_1}^l + C_{S_2}^l) C_T^l] H_T^s H_S^s \right\},
\end{aligned} \tag{A27a}$$

$$\begin{aligned}
b_\theta^{(D^*)}(q^2) &= \frac{G_F^2 |V_{cb}|^2}{128\pi^3 m_B^3} q^2 \sqrt{\lambda_{D^*}(q^2)} \left(1 - \frac{m_\tau^2}{q^2}\right)^2 \\
&\times \left\{ \frac{1}{2} (|\delta_{l\tau} + C_{V_1}^l|^2 - |C_{V_2}^l|^2) (H_{V,+}^2 - H_{V,-}^2) + |\delta_{l\tau} + C_{V_1}^l - C_{V_2}^l|^2 \frac{m_\tau^2}{q^2} H_{V,0} H_{V,t} + 8|C_T^l|^2 \frac{m_\tau^2}{q^2} (H_{T,+}^2 - H_{T,-}^2) \right. \\
&+ \mathcal{R}e[(\delta_{l\tau} + C_{V_1}^l - C_{V_2}^l)(C_{S_1}^{l*} - C_{S_2}^{l*})] \frac{m_\tau}{\sqrt{q^2}} H_S H_{V,0} - 4\mathcal{R}e[(\delta_{l\tau} + C_{V_1}^l) C_T^{l*}] \frac{m_\tau}{\sqrt{q^2}} (H_{T,0} H_{V,t} \\
&+ H_{T,+} H_{V,+} + H_{T,-} H_{V,-}) + 4\mathcal{R}e[C_{V_2}^l C_T^{l*}] \frac{m_\tau}{\sqrt{q^2}} (H_{T,0} H_{V,t} + H_{T,+} H_{V,-} + H_{T,-} H_{V,+}) \\
&\left. - 4\mathcal{R}e[(C_{S_1}^l - C_{S_2}^l) C_T^{l*}] H_{T,0} H_S \right\}.
\end{aligned} \tag{A27b}$$

- [1] J. Lees *et al.* (BABAR Collaboration), *Phys. Rev. Lett.* **109**, 101802 (2012).
- [2] J. Lees *et al.* (BABAR Collaboration), [arXiv:1303.0571](https://arxiv.org/abs/1303.0571).
- [3] A. Matyja *et al.* (Belle Collaboration), *Phys. Rev. Lett.* **99**, 191807 (2007).
- [4] I. Adachi *et al.* (Belle Collaboration), [arXiv:0910.4301](https://arxiv.org/abs/0910.4301).
- [5] A. Bozek *et al.* (Belle Collaboration), *Phys. Rev. D* **82**, 072005 (2010).
- [6] For a review, e.g., J. F. Gunion, H. E. Haber, G. Kane, and S. Dawson, *The Higgs Hunter's Guide*, *Frontiers in Physics* (Addison-Wesley, Reading, MA, 1990).
- [7] S. P. Martin, [arXiv:hep-ph/9709356](https://arxiv.org/abs/hep-ph/9709356).
- [8] W. Hou, *Phys. Rev. D* **48**, 2342 (1993).
- [9] M. Tanaka, *Z. Phys. C* **67**, 321 (1995).
- [10] J. F. Kamenik and F. Mescia, *Phys. Rev. D* **78**, 014003 (2008).
- [11] U. Nierste, S. Trine, and S. Westhoff, *Phys. Rev. D* **78**, 015006 (2008).
- [12] M. Tanaka and R. Watanabe, *Phys. Rev. D* **82**, 034027 (2010).
- [13] S. Fajfer, J. F. Kamenik, and I. Nisandzic, *Phys. Rev. D* **85**, 094025 (2012).
- [14] Y. Sakaki and H. Tanaka, *Phys. Rev. D* **87**, 054002 (2013).
- [15] A. Datta, M. Duraismy, and D. Ghosh, *Phys. Rev. D* **86**, 034027 (2012).
- [16] J. A. Bailey *et al.*, *Phys. Rev. Lett.* **109**, 071802 (2012).
- [17] D. Becirevic, N. Kosnik, and A. Tayduganov, *Phys. Lett. B* **716**, 208 (2012).
- [18] S. Fajfer, J. F. Kamenik, I. Nisandzic, and J. Zupan, *Phys. Rev. Lett.* **109**, 161801 (2012).
- [19] A. Celis, M. Jung, X.-Q. Li, and A. Pich, *J. High Energy Phys.* **01** (2013) 054.
- [20] P. Ko, Y. Omura, and C. Yu, *J. High Energy Phys.* **03** (2013) 151.
- [21] A. Celis, M. Jung, X.-Q. Li, and A. Pich, *J. Phys. Conf. Ser.* **447**, 012058 (2013).
- [22] M. Duraismy and A. Datta, *J. High Energy Phys.* **09** (2013) 059.
- [23] A. Crivellin, C. Greub, and A. Kokulu, *Phys. Rev. D* **86**, 054014 (2012).
- [24] M. Tanaka and R. Watanabe, *Phys. Rev. D* **87**, 034028 (2013).
- [25] P. Biancofiore, P. Colangelo, and F. De Fazio, *Phys. Rev. D* **87**, 074010 (2013).
- [26] I. Dorsner, S. Fajfer, N. Kosnik, and I. Nisandzic, [arXiv:1306.6493](https://arxiv.org/abs/1306.6493).
- [27] W. Buchmüller, R. Ruckl, and D. Wyler, *Phys. Lett. B* **191**, 442 (1987).
- [28] I. Caprini, L. Lellouch, and M. Neubert, *Nucl. Phys.* **B530**, 153 (1998).
- [29] D. Melikhov and B. Stech, *Phys. Rev. D* **62**, 014006 (2000).
- [30] G. Aad *et al.* (ATLAS Collaboration), *J. High Energy Phys.* **06** (2013) 033.
- [31] S. Chatrchyan *et al.* (CMS Collaboration), *Phys. Rev. Lett.* **110**, 081801 (2013).
- [32] A. J. Buras, [arXiv:hep-ph/9806471](https://arxiv.org/abs/hep-ph/9806471).
- [33] Y. Grossman, Z. Ligeti, and E. Nardi, *Nucl. Phys.* **B465**, 369 (1996).
- [34] R. Barate *et al.* (ALEPH Collaboration), *Eur. Phys. J. C* **19**, 213 (2001).
- [35] B. Aubert *et al.* (BABAR Collaboration), *Phys. Rev. D* **77**, 032002 (2008).
- [36] B. Aubert *et al.* (BABAR Collaboration), *Phys. Rev. D* **79**, 012002 (2009).
- [37] K. Abe *et al.* (Belle Collaboration), *Phys. Lett. B* **526**, 258 (2002).
- [38] W. Dungel *et al.* (Belle Collaboration), *Phys. Rev. D* **82**, 112007 (2010).
- [39] M. John, in Workshop on *B* Decay into *D*** and Related Issues (<http://indico.lal.in2p3.fr/getFile.py/access?contribId=6&sessionId=1&resId=0&materialId=slides&confId=1902>).
- [40] A. Keune, Ph.D. thesis, École Polytechnique Fédérale de Lausanne, 2012 [<http://lph.epl.ch/publications/theses/these.an.pdf>].
- [41] Y. Amhis *et al.* (Heavy Flavor Averaging Group Collaboration), [arXiv:1207.1158](https://arxiv.org/abs/1207.1158).
- [42] M. Okamoto *et al.*, *Nucl. Phys. B, Proc. Suppl.* **140**, 461 (2005).
- [43] J. A. Bailey *et al.* (Fermilab Lattice Collaboration, MILC Collaboration), *Proc. Sci., LATTICE2010* (2010) 311 [[arXiv:1011.2166](https://arxiv.org/abs/1011.2166)].
- [44] H.-Y. Cheng, C.-K. Chua, and C.-W. Hwang, *Phys. Rev. D* **69**, 074025 (2004).